Clim. Past Discuss., doi:10.5194/cp-2017-55, 2017
Manuscript under review for journal Clim. Past
Discussion started: 19 April 2017

Climate of the Past Discussions

Simulation of climate, ice sheets and CO_2 evolution during the last four glacial cycles with an Earth system model of intermediate complexity

Andrey Ganopolski[1] and Victor Brovkin[2]

[1]Potsdam Institute for Climate Impact Research (PIK), Potsdam, Germany. ganopolski@pik-potsdam.de
[2]Max Plank Institute for Meteorology, Hamburg, Germany; also a guest scientist at PIK
Correspondence to: Andrey Ganopolski (ganopolski@pik-potsdam.de)

In spite of significant progress in paleoclimate reconstructions and modeling of different aspects of the past glacial cycles, the mechanisms which transform regional and seasonal variations in solar insolation into long-term and global-scale glacial-interglacial cycles are still not fully understood, in particular, for CO_2 variability. Here using the Earth system model of intermediate complexity CLIMBER-2 we performed simulations of co-evolution of climate, ice sheets and carbon cycle over the last 400,000 years using the orbital forcing as the only external forcing. The model simulates temporal dynamics of CO_2, global ice volume and other climate system characteristics in good agreement with paleoclimate reconstructions. Using simulations performed with the model in different configurations, we also analyze the role of individual processes and sensitivity to the choice of model parameters. While many features of simulated glacial cycles are rather robust, some details of CO_2 evolution, especially during glacial terminations, are rather sensitive to the choice of model parameters. Specifically, we found two major regimes of CO_2 changes during terminations: in the first one, when the recovery of the Atlantic meridional overturning circulation (AMOC) occurs only at the end of the termination, a pronounced overshoot in CO_2 concentration occurs at the beginning of the interglacial and CO_2 remains almost constant during interglacial or even decline towards the end, resembling Eemian CO_2 dynamics. However, if the recovery of the AMOC occurs in the middle of the glacial termination, CO_2 concentration continues to rise during interglacial, similar to Holocene. We also discuss potential contribution of the brine rejection mechanism for the CO_2 and carbon isotopes in the atmosphere and the ocean during the past glacial termination.

1. Introduction

Antarctic ice cores reveal that during the past 800 kyr, the atmospheric CO_2 concentration (Petit et al., 1999; Jouzel et al., 2007) varied synchronously with the global ice volume (Waelbroeck et al., 2002; Spratt and Lisiecki, 2016). The most straightforward explanation for this fact is that CO_2 drives glacial cycles together with orbital variations, and the longest, 100-kyr component of the late Quaternary glacial cycles, which is absent in the orbital forcing, is the direct response to CO_2

Clim. Past Discuss., doi:10.5194/cp-2017-55, 2017
Manuscript under review for journal Clim. Past
Discussion started: 19 April 2017

Climate of the Past Discussions

forcing where 100-kyr component is the dominant one. However, simulations with climate-ice sheet models of different complexity (e.g. Berger et al., 1999; Crowley and Hyde, 2008; Ganopolski and Calov, 2011; Abe-Ouchi et al., 2013) show that long glacial cycles (i.e. cycles with typical periodicity of ca. 100 ka) can be simulated with constant CO_2 concentration if the latter is sufficiently low. Moreover, these model simulations show that not only the dominant periodicity, but also the timing of glacial cycles, can be correctly simulated without CO_2 forcing. This fact strongly suggests an opposite interpretation of close correlation between global ice volume and CO_2 during Quaternary glacial cycles – namely that glacial cycles represent a strongly nonlinear response of the Earth system to orbital forcing (Paillard, 1998) while variations in CO_2 concentration are directly driven by ice sheets fluctuations. In turn, CO_2 variations additionally amplify and globalize the direct response of the Earth system to the orbital forcing.

In spite of significant number of studies aimed to explain low glacial CO_2 concentrations (e.g. Archer et al., 2000; Sigman and Boyle, 2000; Watson et al., 2000), the influence of ice sheets on carbon cycle remains poorly understood. It is also unclear how much of CO_2 variations represent the direct response to ice sheets forcing and how much is the results of additional amplification of CO_2 variations through the climate-carbon cycle feedback. Indeed, although radiative forcing of ice sheets contributes about a half to glacial–interglacial variations in global temperature (Brady et al., 2013), most of cooling associated with ice sheets is restricted to the area covered by ice sheets and their close proximity. Thus the direct contribution of ice sheets to glacial ocean cooling is rather limited and therefore the effect of ice sheets on CO_2 drawdown through the solubility effect can explain only a fraction of reduction in glacial CO_2. At the same time, the direct effect of ice sheets on atmospheric CO_2 concentration through ca. 3% changes in the ocean volume and global salinity is rather well understood but works in the opposite direction and leads to glacial CO_2 rise of about 10-20 ppm (Sigman et al., 2000; Brovkin et al., 2007). Another direct effect of ice sheet growth on the carbon cycle through reducing area covered by forest (e.g. Prentice et al., 2011) also operates in the opposite direction. However, several other processes could potentially contribute to glacial CO_2 drawdown through ice sheets growth and related lowering of sea level. One such mechanism is enhanced biological productivity in the Southern Ocean due to the iron fertilization effect (Martin, 1990; Watson et al., 2000). The latter is attributed to enhanced dust deposition over the Southern Ocean seen in the paleoclimate records (Martinez-Garcia et al., 2014; Wolff et al., 2006). At least part of this enhanced deposition is associated with the dust mobilization from exposed Patagonian shelf and glaciogenic dust production related to Patagonian ice cap (Mahowald et al., 1999; Sugden et al., 2009). A number of studies on the effect of iron fertilization suggested a contribution of 10 to 30 ppm to the glacial CO_2 decrease (e.g. Watson et al., 2000; Brovkin et al., 2007). Another effect is related to the brines rejection mechanism, more specifically, to a much deeper penetration of brines produced during sea ice formation in the Southern Ocean during glacial time. The latter is explained by shallowing and significant reduction of the Antarctic shelf area. According to Bouttes et al. (2010) this mechanism, in combination with enhanced stratification of the deep ocean, can contribute up to 40 ppm to the glacial CO_2 lowering.

Apart from the mechanisms mentioned above, many other processes have been proposed to explain low glacial CO_2 concentration. Among them are changes in the ocean circulation (Watson et al., 2015) and an increase in the South Ocean

Clim. Past Discuss., doi:10.5194/cp-2017-55, 2017
Manuscript under review for journal Clim. Past
Discussion started: 19 April 2017

stratification (e.g. Kobayashi et al., 2015), increase in sea ice area in Southern Ocean (Stephens and Keeling, 2000) and a shift in the westerlies (Toggweiler et al., 2006), increase in nutrients inventory or change in the marine biota stoichiometry (Sigman et al., 2000; Wallmann et al., 2016), changes in coral reefs accumulation and dissolution (Opdyke and Walker, 1992), accumulation of carbon in the permafrost regions (Ciais et al., 2012; Brovkin et al., 2016), variable volcanic outgassing (Huybers and Langmuir, 2009) and several other mechanisms. Most of these processes are not directly related to the ice sheets area or volume, and thus should be considered as amplifiers or modifiers of the direct response of CO_2 to ice sheets operating through the climate-carbon cycle feedbacks. Although paleoclimate records provide some useful constraints, the relative role of particular mechanisms at different stages of glacial cycles remains poorly understood. Most studies of glacial-interglacial CO_2 variations performed up to date were aimed at explanation of low CO_2 concentration at the Last Glacial Maximum (LGM, ca. 21 ka). In these studies, both continental ice sheets and the radiative forcing of low glacial CO_2 concentration were prescribed from paleoclimate reconstructions. Only few attempted to explain CO_2 dynamics during part (usually glacial termination) or the entire last glacial cycle with models of varying complexity from simple box-type models (e.g. Köhler et al., 2010; Wallmann et al., 2016), models of intermediate complexity (Brovkin et al., 2012; Menviel et al., 2012), or stand-alone complex ocean carbon cycle models (Heinze et al., 2016). In all these studies, radiative forcing of CO_2 (or total GHGs) was prescribed based on paleoclimate reconstructions. Similarly, ice sheets distribution and elevation were prescribed from paleoclimate reconstructions or simulated but, again, using prescribed radiative forcing of GHGs. Thus in all these studies, CO_2 was treated as an external forcing rather than an internal feedback. Here we for the first time performed simulations of the Earth system dynamics during the past four glacial cycles using fully interactive ice sheet and carbon cycle modelling components, and therefore the only prescribed forcing in this experiment is the orbital forcing.

2. The model and experimental setup

2.1 CLIMBER-2 model description

In this study we used the Earth system model of intermediate complexity CLIMBER-2 (Petoukhov et al., 2000; Ganopolski et al., 2001). CLIMBER-2 includes a 2.5-dimensional statistical-dynamical atmosphere model, a 3-basin zonally averaged ocean model coupled to a thermodynamic sea ice model, the 3-dimensional thermomechanical ice sheet model SICOPOLIS (Greve, 1997), the dynamic model of the terrestrial vegetation VECODE (Brovkin et al., 1997) and the global carbon cycle model (Brovkin et al., 2012). Atmosphere and ice sheets are coupled bi-directionally using a physically based energy balance approach (Calov et al., 2005). Ice sheet model is only applied to the Northern Hemisphere. The contribution of the Antarctic ice sheet to global ice volume change is assumed to be constant during glacial cycles and equal to 10%. The model also includes parameterization of the impact of aeolian dust deposition on snow albedo (Calov et al., 2005; Ganopolski et al., 2010). The CLIMBER-2 model in different configurations has been used for numerous studies of past and

Clim. Past Discuss., doi:10.5194/cp-2017-55, 2017
Manuscript under review for journal Clim. Past
Discussion started: 19 April 2017

future climates, in particular, simulations of glacial cycles (Ganopolski et al., 2010; Ganopolski and Calov, 2011; Willeit et al., 2015; Ganopolski et al., 2016) and carbon cycle operation during the last glacial cycle (Brovkin et al., 2012).

As it has been shown in Ganopolski and Roche (2009), temporal dynamics of the Atlantic meridional overturning circulation (AMOC) during glacial terminations in CLIMBER-2 is very sensitive to the magnitude of freshwater flux. To explore different possible deglaciation evolutions, together with the standard model version, we performed an additional suit of simulations where the component of freshwater flux into the ocean originated from melting of ice sheets was uniformly scaled up or down by up to 10%. This rather small change in the freshwater forcing (typically smaller than 0.02 Sv) does not affect AMOC dynamic appreciably during most of time but does induce a strong impact during deglaciations (see below). Other modifications of the climate-ice sheet component of the model are described in the Appendix.

The carbon cycle component used in this study incorporates several modifications compared to our previous studies with CLIMBER-2. Similar to Brovkin et al. (2012), the efficiency of nutrients utilization in the Southern Ocean is set to be proportional to the dust deposition rate, which in the case of one-way coupling is prescribed to be proportional to the dust deposition in EPICA ice core. However, in the fully coupled experiment, the dust deposition rate over the Southern Ocean has been computed from simulated sea level (see Appendix). This means that in the fully interactive run (see below) we did not use explicitly any paleoclimate data to drive the model and the orbital forcing was the only driver of the Earth system dynamics. In the marine carbon cycle component, we also account for a dependence of the remineralization depth on ocean temperature following Segschneider and Bendtsen (2013) (see Appendix). In the previous studies, remineralization depth was kept constant.

The CLIMBER-2 model used in earlier studies of glacial carbon cycle did not include long-term terrestrial carbon pools such as permafrost carbon, peat and carbon buried beneath the ice sheets. In the present version of the model these pools are included. The model also accounts for peat accumulation. Modification of the terrestrial carbon cycle components is described in detail in the Appendix. For simulation of atmospheric radiocarbon during the last glacial termination we used the rate of ^{14}C production following scenario by Hain et al. (2014) which is based on the production model by Kovaltsov et al. (2012).

2.2 One-way coupled and fully interactive experiments

In our previous experiments performed with the CLIMBER-2 model (Brovkin et al., 2012; Ganopolski and Brovkin, 2015) we not only prescribed temporal variations in the Earth's astronomical parameters (eccentricity, precession and obliquity) but also the radiative effect of GHGs (CO_2, CH_4 and N_2O) computed using their concentrations from the ice cores records (Luthi et al., 2008; Petit et al., 1999). In these experiments, which we will denote hereafter as "one-way coupled" (Fig. 1a, Table 1), atmospheric CO_2 was computed by the carbon cycle module but not used as the radiative forcing for the climate component. Similarly, in these experiments CO_2 fertilization effect on vegetation was computed using reconstructed CO_2 concentration. Therefore in one-way coupled experiments there were no feedbacks of the simulated atmospheric CO_2

Clim. Past Discuss., doi:10.5194/cp-2017-55, 2017
Manuscript under review for journal Clim. Past
Discussion started: 19 April 2017

concentration to climate. In the present study, we performed a suit of one-way coupled experiments for the last four glacial cycles but we also performed fully interactive simulations in which the orbital forcing was the only prescribed external forcing. Since CLIMBER-2 does not include methane and N_2O cycles and does not account for these GHGs in its radiative scheme, we made use of the fact that CO_2 is the dominant GHG and that temporal variations of other two follow rather closely CO_2. To account for the effect of methane and N_2O forcings, we computed the effective CO_2 concentration used in the radiative scheme of the model in such a way that radiative forcing of equivalent CO_2 exceeds radiative forcing of simulated CO_2 by 30% at any time. This type of experiments we will refer to as "fully interactive" (Fig. 1b). In the fully interactive experiment we use computed CO_2 concentration also in terrestrial component to account for CO_2 fertilization effect. As was stated above, dust deposition over the Southern Ocean used in the parameterization of iron fertilization effect computed from the global sea level. The radiative forcing of aeolian dust and dust deposition on ice sheets (apart from the glaciogenic dust sources) in both types of experiments were obtained identically to Calov et al. (2005) and Ganopolski and Calov (2011) by scaling the field computed with GCMs, where scaling parameter was proportional to global ice volume.

2.3 Model spin-up

The model spin-up and proper choice of model parameters for simulation of multiple glacial cycles represent a challenge when using the models with very long-term components of the carbon cycle because inconsistent initial conditions or even a small disbalance in carbon fluxes could lead to a large drift in simulated atmospheric CO_2 concentration (in the case of one-way coupling) or the state of the entire Earth system (climate, ice sheets, CO_2) in the case of fully interactive experiments. Note that in the latter case, the negative climate-weathering feedback will eventually stabilize the system but this occurs at the time scale of several glacial cycles and over this time climate could drift far away from its realistic state. To avoid such drift, volcanic outgassing should be carefully calibrated. Based on a set of sensitivity experiments, we found that the value of 5.3 Tmol C/yr allows us to simulate quasiperiodic cycles without long-term trend in atmospheric CO_2. Note, that even ±10% change in volcanic outgassing leads to significant (order of 100 ppm) drift in CO_2 concentration simulated over the last four glacial cycles.

When the carbon cycle model incorporates such long-term processes as terrestrial weathering, marine sediment accumulation and permafrost carbon burial, the assumption that the system is close to equilibrium at preindustrial period or at any other moment of time is not valid even if CO_2 concentration was relatively stable during a certain time interval. To produce proper initial conditions at 410 ka we performed a sequence of 410 ky-long one-way coupled runs with the identical forcings. We first used as the initial conditions the final state obtained in simulation of the last glacial cycles (Brovkin et al., 2012). Then we launched each 410 ky experiment from the final state obtained in the previous model run. The results of such sequence of experiments reveal a clear tendency to converge to the solution with similar initial and final states of the Earth system. We then used the state of climate and carbon cycle obtained at the end of the last run as the initial conditions for all

Clim. Past Discuss., doi:10.5194/cp-2017-55, 2017
Manuscript under review for journal Clim. Past
Discussion started: 19 April 2017

experiments presented in this paper. In the analysis of all experiments described below we exclude the first 10,000 years when adaptation of different fields to each other occurs.

3. Simulations of the last four glacial cycles

Realistic simulation of climate and carbon cycle evolution during the last four glacial cycles is more challenging in the case of fully interactive configuration, because in this case a number of additional positive feedbacks tend to amplify initial model biases. Therefore we begin our analysis with the one-way coupled simulations similar to that performed in Brovkin et al. (2012). This configuration was also used for calibration of new parameterizations (see section 4) and sensitivity experiments for the last glacial termination (section 5).

3.1 Experiments with one-way coupled climate-carbon cycle model

Simulated climate and ice sheets evolution in the one-way coupled experiments are rather similar to the ones in Ganopolski and Calov (2011), which is not surprising since the only difference between model versions used in these studies is related to the coupling between ice sheet and climate components (see Appendix). Simulated glacial cycles are characterized by global surface air temperature variations of about 5^{o}C (not shown) and maximum sea level drops by more than 100 meters during several glacial maxima. Simulated global ice sheets volume during most of time is close to the reconstructed one (Spratt and Lisiecki, 2016) (Fig. 2d). In general, differences between simulated and reconstructed global sea level are comparable or smaller than uncertainties in sea level reconstructions obtained using different methods.

Simulated CO_2 concentration (Fig. 2e) is also in a good agreement with reconstructions based on several Antarctica ice cores (Barnola et al., 1987; Monnin et al., 2004; Petit et al., 1999; Luthi et al., 2008). The model correctly reproduces the magnitude of glacial-interglacial CO_2 variability of about 80 ppm. Results of simulations with the standard model version (ONE_1.0) and model with 10% enhanced meltwater flux (ONE_1.1) are essentially identical during most of time except for glacial terminations. During glacial terminations even rather small differences in the freshwater forcing cause pronounced differences in the temporal evolution of the AMOC, and as a result, of CO_2 concentration. As seen in Fig. 2d, in the experiment ONE_1.0, CO_2 concentration grows monotonously during the last glacial termination (TI, midpoint at ca. 15 ka) and TIV (ca. 330 ka) while it rises faster and overshoots the interglacial level during TII (ca. 135 ka) and TIII (ca. 240 ka). To the contrary, in the experiments ONE_1.1, similar overshoots occur during TI and III but not TIV. In all cases, simulated CO_2 lags behind the reconstructed one but this lag is smaller in the case when overshoot is simulated. Experiments with CO_2 overshoots are clearly in better agreement with empirical data for MIS7 and MIS9. Analysis of model results shows that pronounced CO_2 overshoot occurs in the case when the AMOC is suppressed during the entire glacial termination and recovers only after the cessation of the meltwater flux (Fig. 3). To the contrary, if the AMOC recovers well before the end of deglaciation, simulated CO_2 experiences only local overshoot and continues to rise during most of the interglacial. The latter

Clim. Past Discuss., doi:10.5194/cp-2017-55, 2017
Manuscript under review for journal Clim. Past
Discussion started: 19 April 2017

behaviour is similar to that was observed during MIS 11 and the Holocene, while the former is typical for MIS5, 7 and 9. Thus our model is able to reproduce both types of CO_2 dynamics during the interglacials.

Comparison of simulated deep ocean $\delta^{13}C$ with paleoclimate reconstructions (Fig. 4) show that the model correctly simulates larger $\delta^{13}C$ variability in the deep Atlantic in comparison to the deep Pacific but underestimates the amplitude of glacial-interglacial $\delta^{13}C$ variability. Simulated atmospheric $\delta^{13}CO_2$ shows a rather complex behaviour and amplitude of variability up to 0.6‰. More detailed comparison with empirical data during the last deglaciation is presented in the Section 5.

3.2. Experiments with the fully interactive model

In two-way coupling experiments (fully interactive runs), orbital forcing is the only prescribed forcing and the model does not use any time-dependent paleoclimatological information (such as the Antarctic dust deposition rate used in the one-way coupled experiment). Results of fully interactive experiment INTER_1.0 are shown in Fig. 5. For the first experiment of this type ever, the agreement between model simulations and empirical reconstructions is reasonably good. The model simulates correct magnitude and timing of the last four glacial cycles both in respect of sea level and CO_2 concentration. It also reproduces strong asymmetry of glacial cycles. Naturally, the mismatch between simulated and reconstructed characteristic in fully interactive experiments is larger than in the one-way coupled experiment. In particular, in fully interactive experiment, simulated ice volume is underestimated by 10-20 meters compared to reconstructed one. Although the magnitude of glacial-interglacial CO_2 variability in the fully interactive experiment INTER_1.0 is similar to that in one-way coupled experiment ONE_1.0 and in reconstructions, the lag between simulated and reconstructed CO_2 during glacial terminations increases additionally in comparison to one-way coupled experiment. Interestingly, the last glacial cycle and the first 150 ky of the INTER_1.0 and ONE_1.0 runs are in very good agreement while during time interval between 300 ka and 150 ka BP discrepancies are larger. This period corresponds to higher eccentricity and therefore larger magnitude of the orbital forcing. Similarly to the results of one-way coupled experiments, fully interactive runs also show strong sensitivity to magnitude of freshwater flux during glacial terminations.

Comparison of simulated ice sheets spatial distribution and elevation (Fig. 6) shows that the results of one-way coupled (ONE_1.0, Fig 6a) and fully interactive run (INTER_1.0, Fig. 6b) are almost identical during the LGM (the same is true for the previous glacial maxima, not shown) and in a reasonable agreement with the paleoclimate reconstructions. During glacial terminations, the difference between two runs increases since in the fully interactive run the radiative forcing of GHGs lags considerably behind the reconstructed one used in the one-way coupled experiment. As the result at 7 ka continental ice sheets melted completely in the one-way coupled experiment (Fig. 6c) while in the fully interactive run a relatively large ice sheet is still present in the northern-eastern Canada (Fig. 6d).

Clim. Past Discuss., doi:10.5194/cp-2017-55, 2017
Manuscript under review for journal Clim. Past
Discussion started: 19 April 2017

It is instructive to compare frequency spectra of simulated and reconstructed global ice volume in one-way and fully coupled experiments (Fig. 7). In addition, we show here results from the experiment ONE_240 performed with constant radiative forcing of GHGs corresponding to equivalent CO_2 concentration of 240 ppm. As already shown by Ganopolski et al. (2011), even with constant CO_2, the model computes pronounced glacial cycle with 100-kyr periodicity, although it has much weaker amplitude than the reconstructed sea level. Both model experiments with varying CO_2 radiative forcing (ONE_1.0 and INTER_1.0) reveal much stronger 100-kyr periodicity, which has only slightly weaker amplitude than the spectrum of reconstructed sea level. Interestingly, frequency spectra of sea level simulated in one-way and fully interactive runs have rather similar power in 100 ka and obliquity (40 ka) bands, but in the precessional band (ca. 20 ky) one-way coupled experiment reveals much higher spectral power. This cannot be explained by the prescribed radiative forcing of GHGs because the latter contains very little precessional variability. The explanation of stronger precessional component in the ONE_1.0 run is related to the fact that one-way coupled model simulates slightly faster ice sheet growth during initial part of each glacial cycle and the modeled sea level variability at the precessional frequency is very sensitive to the ice volume.

4. The composition of "the carbon stew" and factor analysis

In this section, we discuss the contribution of different factors to simulated variations in CO_2 concentration. Because neither of mechanisms could explain the CO_2 dynamics in isolation from the other factors (e.g. Sigman and Boyle, 2000; Archer et al., 2000), we call the composition and timing of the mechanisms leading to the glacial CO_2 cycle "the carbon stew". Similar to the study by Brovkin et al. (2012), we performed a set of experiments using one-way coupling (see Table 1 for detail). We use this approach instead of fully interactive coupling to exclude complex and strongly nonlinear interactions associated with ice sheet dynamics which significantly complicate factor analysis. In the case of one-way coupled experiments climate, ice sheets and other external factors are identical and experiments only differ by parameters of the carbon cycle model. Since CO_2 simulated in the one-way coupled experiment with 10% enhanced meltwater flux (ONE_1.1) is in better agreement with observational data than the standard one (ONE_1.0), for the factor analysis we used experiment ONE_1.1 as the reference one and performed all sensitivity experiments with 10% enhanced meltwater flux.

4.1 The standard carbon cycle model setup

We begin our analysis from the experiment that incorporates only standard ocean biogeochemistry as described in Brovkin et al. (2007) (Fig. 8). This experiment does not include effect of terrestrial carbon cycle. In this configuration, the model is able to explain only about 40 ppm of CO_2 reduction during glacial cycles. Note that this experiment accounts for changes in the ocean volume by ca. 3% and corresponding changes in the total biogeochemical inventories including salinity. These volume changes are often neglected in simulations with 3-dimensional ocean models (e.g. Heinze et al. 2016),

Clim. Past Discuss., doi:10.5194/cp-2017-55, 2017
Manuscript under review for journal Clim. Past
Discussion started: 19 April 2017

although in our simulations they counteract to glacial CO_2 drawdown by up to 20 ppm. Accounting for the land carbon changes does not help to explain the CO_2 concentration changes, since terrestrial carbon contains by ca. 350 Gt carbon less at the LGM compared to the pre-industrial state. This reduces the glacial-interglacial CO_2 difference by 10-20 ppm comparing to the ocean-only experiment (Fig. 8b). Enabling of parameterization for the iron fertilization effect in the Southern Ocean results in additional glacial CO_2 drawdown of up to 30 ppm, mostly towards the end of each glacial cycle which is related to the chosen parameterization for the dust deposition rate (Fig. 8c). With all these processes considered in our previous study by Brovkin et al. (2012), we are still short of ca. 20 ppm to explain the full magnitude of glacial-interglacial variability.

4.2 Additional processes included in the carbon cycle model

There is a number of other proposed mechanisms which can explain several tens ppm of glacial CO_2 decline. Our choice of two processes to obtain the observed magnitude of glacial-interglacial CO_2 variations is somewhat subjective. Chosen mechanisms are explained below, while an alternative one (brine rejection) is discussed in the section 4.3.

The first additional to Brovkin et al. (2012) mechanism is temperature-dependent remineralization depth. In the standard CLIMBER-2 version, remineralization depth is spatially and temporally constant. Since in the colder ocean remineralization depth increases, this enhances the efficiency of carbon pump and contributes to a decrease of atmospheric CO_2 concentration (e.g. Heinze et al., 2016; Menviel et al., 2012). Details of the mechanism implementation are described in Appendix. As seen from Fig. 8e, making remineralization depth temperature-dependent introduces additional glacial-interglacial variability with the magnitude of about 20 ppm. Roughly half of this value is clearly attributed to the CO_2 overshoots which are seen at the beginning of some interglacials. The reason is that the AMOC shutdowns due to melt water flux that happened during glacial terminations lead not only to surface cooling in the North Atlantic, but also to significant thermocline warming that occurs over the entire Atlantic ocean (e.g. Mignot et al., 2007). This subsurface warming causes significant shoaling of the remineralization depth and the release of carbon from the ocean into the atmosphere. This process reverses after the recovery of the AMOC at the beginning of interglacials.

Burley and Katz (2015) and Huybers and Langmuir (2009) proposed that the rate of volcanic outgassing varies during glacial cycle due to variable load of the ice sheet and ocean on the Earth crust. Therefore we assume that volcanic outgassing has a variable component (about 30% of its averaged value of 5.3 Tmol/yr) which represent the delayed response to the change in ice volume. This simple parameterization explained in Appendix does not affect cumulative volcanic outgassing over glacial cycle, but contributes to glacial-interglacial variability by additional 10 ppm (Fig. 8d). With varying volcanic outgassing and temperature-dependent mineralization depth, CLIMBER-2 model reproduces glacial-interglacial CO_2 cycles in a good agreement with paleoclimate records (Fig. 8a, blue line).

Clim. Past Discuss., doi:10.5194/cp-2017-55, 2017
Manuscript under review for journal Clim. Past
Discussion started: 19 April 2017

4.3 Brine rejection mechanism

Using a different version of CLIMBER-2, Bouttes et al. (2010) proposed that a significant fraction of glacial-interglacial CO_2 variations can be explained by the mechanism of brine rejections, more specifically, by a large increase in the depth to which brines can penetrate under glacial conditions without significant mixing with ambient water masses. Such increase in brine efficiency under glacial conditions would result in large transport of salinity, carbon and other tracers from the upper ocean layer into the deep ocean. By choosing the efficiency coefficient close to one, Bouttes et al. (2010) demonstrated that brines are able to explain up to 40 ppm CO_2 decrease. We have implemented this mechanism in combination with stratification-dependent vertical diffusivity in our version of the CLIMBER-2 model and got results qualitatively similar to Bouttes et al. (2010).

While we think that the brine rejection mechanism belongs to a class of plausible mechanisms contributing to glacial CO_2 drawdown, we did not use brine parameterization in our simulations for several reasons. Firstly, the parameterization for brine rejection cannot be tested against observational data. For present day climate conditions, brine rejections efficiency should be below 0.1, otherwise modern Antarctic bottom water becomes saltier than the North Atlantic deep water which is in odd with reality. This means that to be efficient mechanisms for glacial CO_2 drawdown, the brine efficiency should increase under glacial conditions at least by order of magnitude. Whether this is physically plausible is not clear. The only paleoclimate constraint on the brine efficiency is reconstruction of paleosalinity based on the pore water (Adkins, et al. 2002) which suggests increase of deep water salinity in the Southern Ocean by more than 2 psu during the LGM. Such increase in salinity is indeed difficult to reproduce without contribution of brines. However the accuracy of salinity reconstruction based on such method remains uncertain (Wunsch, 2016). Second, there is a problem with temporal dynamics of brine rejection efficiency. Mariotti et al. (2016) assumed abrupt decrease of brine rejection efficiency from 0.7 to 0 in a very short interval between 18 and 16 ka. However, both sea level and the size of Antarctic ice sheets were essentially constant during this period and therefore there is no obvious reason for such large variations in the brine rejection efficiency. According to the interpretation of Roberts et al.(2016), brines rejection remained efficient during most of glacial termination and ceased only after 11 ka when most of glacial-interglacial CO_2 rise has been already accomplished. In the view of these uncertainties, we decided not to include parameterizations of brine rejection mechanism in simulations of glacial cycles. However, for simulations of the last glacial termination discussed below, we analysed potential effect of brine rejection on radiocarbon and other paleoclimate proxies.

5. Simulations of the Termination I

5.1 Simulation of climate, CO_2, and carbon isotopes during the last termination

Clim. Past Discuss., doi:10.5194/cp-2017-55, 2017
Manuscript under review for journal Clim. Past
Discussion started: 19 April 2017

The last glacial termination provides a wealth of paleoclimate records with a potential to better constrain the mechanisms of glacial CO_2 variability. In this section, we discuss the last glacial terminations in more detail. Similarly to the previous section, to exclude nonlinear interaction with ice sheets, we discuss here only one-way coupled experiments. To reduce computational time, we performed experiments only for the last 130,000 years starting from the Eemian interglacial and using the same initial conditions as in the experiments discussed above.

In the standard ONE_1.0_130K experiment, the model simulates climate variability across the Termination I rather realistically. In particular, it reproduces temporal resumption of the AMOC in the middle of the termination resembling Bolling-Allerod warm event (Fig. 9a). The timing of this event in our model is shifted by ca 1000 years compared to the paleoclimate records. Results of our experiments reveal a high sensitivity of the timing of the AMOC resumption to the magnitude of freshwater flux. A change of the flux by just 2% in the ONE_0.98_130K experiment significantly alters millennial scale variability during the last glacial termination (Fig. 9). This result suggests that simulated millennial scale variability during the Termination I is not robust, i.e. it is unlikely that a single model run through the glacial termination would reproduce the right timing or even the right sequence of millennial-scale events.

Although simulated CO_2 concentration at LGM and pre-industrial state are close to observations, simulated CO_2 appreciably lags behind reconstructed CO_2 during the termination (Fig. 9b). This is primarily related to the fact that simulated CO_2 does not start to grow at ca. 18 ka BP as reconstructed, but only after the end of simulated analogue of Bolling-Allerod event. At the same time, in agreement with paleoclimate reconstructions, CO_2 concentration reaches a local maximum at the end of cold event, which resembles the Younger Dryas. Simulated CO_2 concentration also reveals continuous CO_2 rise during Holocene towards preindustrial value of 280 ppm. This result confirm that such CO_2 dynamics could be explained by only natural mechanisms and does not require early anthropogenic CO_2 emissions until ca. 2 ka (Kleinen et al., 2016). This result also demonstrates that temporal dynamics of CO_2 during interglacials critically depends on the timing of final AMOC recovering. Late recovery causes strong overshoot of CO_2 at the beginning of interglacial following by some decrease or stable CO_2 concentration. At the same time earlier AMOC recovery causes only temporal CO_2 overshoot and leads to continuous CO_2 rise during interglacial.

It is assumed that atmospheric $\delta^{13}C$ provides useful constraint on the mechanisms of deglacial CO_2 rise (Schmitt et al., 2012; Joos et al., 2004; Fischer et al., 2010). Simulated atmospheric $\delta^{13}C$ drops from the LGM level of about -6.4‰ to the minimum value of -6.7‰ between 16 and 14 ka (Fig. 9c). This is primarily related to the reduction of marine biological productivity which, in turn, is explained by the decrease of iron fertilization effect over the Southern Ocean during the first part of Termination I. The magnitude of the $\delta^{13}C$ drop is in a good agreement with empirical data (Fig. 9c). The model is also able to simulate W-shaped $\delta^{13}C$ evolution associated with reorganization of the AMOC. $\delta^{13}C$ rise after 12 ka is primary attributed to the accumulation of carbon in terrestrial carbon pools (forest regrowth and peat accumulation). At the same time, simulated present-day atmospheric $\delta^{13}C$ is underestimated compared to ice-core data by ca. 0.2‰.

Clim. Past Discuss., doi:10.5194/cp-2017-55, 2017
Manuscript under review for journal Clim. Past
Discussion started: 19 April 2017

The model simulates almost monotonous decrease of atmospheric $\Delta^{14}C$ from the LGM to present. Most of this decrease (ca. 200‰) is caused by prescribed production rate which was about 20% higher during LGM. Only about 80 ‰ of $\Delta^{14}C$ is attributed to difference in climate state between LGM and present, primarily, due to less ventilated deep ocean. As shown in Fig. 9d, simulated atmospheric $\Delta^{14}C$ is significantly underestimated before 12 ka compared to reconstruction by Reimer et al. (2013) and at LGM this difference reaches more than 100‰. It is possible but unlikely that such big differences can be attributed to uncertainties in reconstructed production rate. Alternative hypothesis for explaining this mismatch is discussed below.

Fig. 10 shows the LGM time slice anomalies and temporal evolution of ^{13}C and ^{14}C during the Termination I in the Atlantic ocean. Spatial distribution of glacial anomalies and temporal dynamics of both carbon isotopes during termination are qualitatively very similar. Both show pronounced response at all depth to the millennial scale reorganization of the AMOC. Glacial $\delta^{13}C$ in the deep Atlantic at the LGM is by 0.6-1‰ lower than at present; that is primarily related to shoaling of the AMOC and reduced ventilation in the Southern Ocean. At the LGM, a difference between ^{14}C is the upper ocean layer and at given depth, $\Delta\Delta^{14}C$, reaches ca 200‰ that corresponds to relative (to the upper layer) reservoir age of about 2000 years. This is in good agreement with Roberts et al.(2016). Both carbon isotopes show little changes during Holocene.

5.2 Brine rejection mechanisms and radiocarbon in the ocean and atmosphere

As discussed above, our version of the CLIMBER-2 model is not able to reproduce accurately atmospheric ^{14}C decline during the first part of glacial termination. At the same time, Mariotti et al. (2016) demonstrated that their version of CLIMBER-2, which incorporates mechanism of brine rejection, is able to simulate larger atmospheric ^{14}C decrease from LGM till present, consistently with observational data (Reimer et al., 2013). By introducing similar parameterization for brine rejection and stratification-dependent vertical diffusivity in our model, we are able to reproduce results similar to Mariotti et al. (2016) (Fig. 11). It is noteworthy that we use different temporal dynamics of the efficiency of brine rejections during termination. Instead of abrupt and non-monotonous changes in the brine efficiency prescribed in Mariotti et al. (2016), in the ONE_BRINE_130K experiment we assume that this efficiency is 0.75 at the LGM, 0 at present, and in between it follows global ice volume. We do not claim that this scenario is more realistic, but at least it is more consistent with the findings of Roberts et al. (2016). Fig. 10 shows that the model with brine rejection and stratification-dependent vertical diffusivity simulates atmospheric $\Delta^{14}C$ in better agreement with empirical data then the standard version. This is explained by the fact that brine rejection in combination with stratification-dependent vertical mixing produces very salty and dense deep water masses which are almost completely isolated from the surface. In response, $\Delta\Delta^{14}C$ in the deep Atlantic drops below -400‰ (in Mariotti et al. (2016) it drops even below -500‰). Such low $\Delta\Delta^{14}C$ corresponds to relative (to the surface) ventilation age of 3000 to 4000 years both in Atlantic and Pacific. Similar ventilation age values simulated for South Ocean and deep Pacific (Fig. 12b) are much older than suggested by Freeman et al. (2016). Interestingly, the two model

Clim. Past Discuss., doi:10.5194/cp-2017-55, 2017
Manuscript under review for journal Clim. Past
Discussion started: 19 April 2017

versions do not differ much in respect of simulated deep ocean $\delta^{13}C$. At last, the two model versions differ significantly in respect of the deep South Ocean salinity. Change in salinity in the standard model version is only about 1 psu which is close to the global mean salinity change due to ice sheets growth. The model version with the brine rejection parameterization simulates glacial deep South Ocean salinity of above 37 psu which is in a good agreement with the reconstruction by Adkins et al. (2002). Thus we found that including additional effects (brines and stratification-dependent diffusion) helps to bring atmospheric $\Delta^{14}C$ and the deep South Ocean salinity in better agreement with available reconstructions but in expense of very old (likely to be in odd with paleoclimate data) water masses in the deep ocean. Of course, these results are obtained with a very simplistic ocean component and it is possible that more realistic ocean models would be able to resolve this apparent contradiction.

5.3 Changes in the terrestrial carbon cycle

The evolution of the carbon cycle in the "offline" simulation is presented on Figure 13. The "conventional" components of the land carbon cycle (vegetation biomass, soil carbon stored in non-frozen and non-flooded environment) change between 1400 GtC during glacial maxima and 2000 GtC during interglacial peaks. Such an amplitude of 600 GtC of glacial-interglacial changes is typical for the models of the land carbon cycle without long term-components (Kaplan et al., 2002; Joos et al., 2004; Brovkin et al., 2002). However, when we account for permafrost, peat, and buried carbon, the magnitude is decreasing to 300-400 GtC. This is due to counteracting effect of the permafrost and buried carbon pools relative to the conventional components. Both these pools vary between 0 and 350 GtC and reach their maxima during glacials. The peat storage also reaches about 350 GtC, but it grows only during interglacials or warm stadials. Let us note that during glacial inceptions, while biomass and mineral soil carbon decrease, terrestrial carbon storage increases due to an increase in buried and permafrost carbon. As a result, total land carbon did not change much during the period of large ice sheet initiation.

During the last deglaciation (Fig. 13, right), the peat storages increase monotonically reaching ca. 350 GtC at pre-industrial. The conventional carbon pools increase from 1400 to 1800 GtC at the peak of interglacial (ca. 9 kyr BP), and then start to decline due to orbital forcing effect on climate in northern hemisphere. The permafrost and buried carbon pools show opposite behaviour, experiencing minimum at 10 and 5 ka, respectively, and grow afterwards. The combined effect on the total land carbon is a monotonic increase during interglacials, mostly because of peat accumulation.

6. Conclusions

We present here the first simulations of the last four glacial cycles with one-way and two-way coupled carbon cycle model. The model is able to reproduce the major aspects of glacial-interglacial variability of climate, ice sheets and of atmospheric CO_2 concentration even when driven by orbital forcing alone. In particular, the model simulates correct timing of glacial terminations and dominant 100-kyr cyclicity of the past glacial cycles.

The model correctly simulates climate and carbon cycle evolution across the last glacial terminations. In particular, ocean carbon isotopes evolution is simulated in agreement with empirical data. At the same time, simulated CO_2 lags behind reconstructed one during glacial termination and the magnitude of atmospheric ^{14}C is underestimated. Introducing brine rejection parameterization and stratification-dependent diapycnal diffusivity allows us to improve agreement for the atmospheric ^{14}C but leads to unrealistically "old" deep ocean water masses.

Temporal dynamics of CO_2 during interglacial depends strongly on the timing of the AMOC recovering during glacial termination. If the AMOC recovers only at the end of glacial termination, CO_2 concentration experiences the overshoot at the beginning of interglacial and then CO_2 declines. To the contrary, early recovery of the AMOC, leads to monotonous rise of CO_2 during interglacials.

Glacial termination similar to the Termination I is not robust. The sequence and timing of millennial scale events are very sensitive to magnitude of meltwater flux.

Adding new long-term carbon pools (peat, buried and permafrost carbon) decreases an amplitude of glacial-interglacial changes in land carbon storages. It helps to reduce an effect of terrestrial biosphere on the CO_2 change during glacial inception and to lesser extent during glacial terminations.

Acknowledgements. The authors are thankful to Edouard Bard and Fortunat Joos for helpful discussion of the atmospheric and oceanic ^{14}C dynamics. The authors acknowledge support by the German Ministry of Education and Research (PalMod-Project)

Clim. Past Discuss., doi:10.5194/cp-2017-55, 2017
Manuscript under review for journal Clim. Past
Discussion started: 19 April 2017

Climate of the Past Discussions

Appendixes

A1. Modifications of terrestrial carbon cycle model

The old version of the CLIMBER-2 carbon cycle module described in Brovkin et al (2002) considers two vegetation types – trees and grass. Each of two vegetation types has four carbon pools – leaves, stems, fast and slow soil carbon. Each of these four pools occupies the same fraction of grid cell as the respective vegetation type. Crichton et al. (2014) in their version of permafrost carbon implementation into CLIMBER-2 have not changed the pool structure but modified turnover time, assuming that it is increasing under permafrost conditions. In the new version of the carbon cycle module which we use in present work, we introduced three new carbon pools: boreal peat, permafrost, and carbon buried under ice sheets (Fig. A1). The fractions of land covered by grass and trees are computed in the vegetation model following (Brovkin et al., 1997), the fraction of land covered by ice sheets is computed by the ice sheet model and the fraction of permafrost f_{pm} for the temperature range -5°C < T_{ts} < 5°C is computed in the land surface module as

$$f_{pm} = 0.5 - 0.1T_{ts},$$

where T_{ts} is annual mean top soil layer temperature. It is assumed that grass (in boreal latitudes this mean tundra) is located north of forest and therefore freezes first. Only if permafrost exceeds grass fraction, the permafrost can expand over the area covered with trees. During the ice sheet growth, all carbon under ice sheets apart from the living biomass is re-allocated into the buried carbon pool. Buried carbon remains intact till it is covered by ice sheets. During deglaciation, this buried carbon is transformed into the permafrost pool. Fraction of land covered by peat is define as

$$f_{pt} = f_{pt}^{*}(1 - f_{gc} - f_{pm}),$$

where f_{pt}^{*} is the potential fraction of peat for each grid cell prescribed from modern observational data and f_{gc} id the faction of land covered by ice sheets. Note that we do not consider peatlands in low latitudes. Although peat and permafrost have certain areal fractions, they are considered to be parts of grid cell covered by vegetation. Net primary production and fluxes between the fast carbon pools (leaves, stems and fast soil pool) are computed the same way as in Brovkin et al. (2012). The downward flux of carbon from the fast soil is partitioned between slow soil pool and permafrost proportionally to their relative factions. The rate of peat accumulation is equal to a fixed fraction of net primary production in the respective vegetation type. Evolution of carbon content p_i in slow carbon pools is described by the equation

Clim. Past Discuss., doi:10.5194/cp-2017-55, 2017
Manuscript under review for journal Clim. Past
Discussion started: 19 April 2017

$$\frac{dp_i}{dt} = q_i f_i + \frac{df_i}{dt} b_i' ,$$

where $p_i = b_i f_i$, and b_i is the concentration of carbon in the *i*-th carbon pool (in kgC/m^2), and f_i is the fraction of the *i*-th pool. Value q_i represents the difference between local accumulation and decay of carbon in the pool, and b_i' is carbon concentration in the pool by which *i*-th pool is expanded and $b_i' = b_i$ if *i*-th pool is shrinking. For peat $b_i' = 0$. For the permafrost, the situation is more complex, because it can gain/lost carbon from/to slow soil, peat and buried carbon pools. The source terms for the permafrost pool q_{pm} consists of the sum of fluxes from the fast grassland and tree fast soil pools into the respective slow pools (see Brovkin et al., 2002 for detail) minus the decay term, where decay time scale is set to 20,000 years. Apart from carbon, terrestrial carbon model also computes carbon isotopes (^{13}C and ^{14}C) contents in all carbon pools. Since carbon isotopes are also computed in the oceanic carbon cycle model, we can compute δ^{13}C and δ^{14}C in the atmosphere and compare modeling results with available paleoclimate data.

A2 Modifications of the ocean carbon cycle module

A2.1. Dust deposition in the Southern Ocean

In the one-way coupled experiments, similar to Brovkin et al. (2012), we used the concentration of eolian dust in the Antarctic ice cores as the proxy for iron deposition over the Southern Ocean. Such choice is supported by recent measurements of iron content in the Southern Ocean sediments core (Lamy et al., 2014). In the fully interactive run, the iron flux over the Southern Ocean (*D*) in arbitrary units is parameterized through the global sea level change as

$$D = (100\frac{dS}{dt} + 10)\max(S - 50;\, 0) + 1.5S ,$$

where *S* is the ice volume expressed in meters of sea level equivalent and time *t* is in years. This formula gives significant increase in iron flux for the case when sea level drops below 50 m, that is likely related to the fact that Patagonian dust source is very sensitive to the area of exposed shelf and glacial erosion processes. Numerical parameters in this formula were obtained by fitting simulated *D* to the dust concentration in Antarctic record. This allows us to use the same parameterization for the iron fertilization effect in one-way and fully interactive experiments. To prevent large fluctuations in the iron flux related to fluctuations of time derivative of *S*, the dust deposition *D* computed by this equation has been smoothed by applying relaxation procedure. Namely, at each time step *n*, the dust deposition D_n is computed as

Clim. Past Discuss., doi:10.5194/cp-2017-55, 2017
Manuscript under review for journal Clim. Past
Discussion started: 19 April 2017

$$D_n = (1-\varepsilon)D + \varepsilon D_{n-1}$$

Where ε=0.001 which is approximately equivalent to introducing of 1000 years filter.

A2.2 Dependence of remineralization depth on temperature

In CLIMBER-2 the vertical profile of carbon below the euphotic zone is given by the formula

$$f(z) = \left(\frac{z}{z_r}\right)^{0.858}$$

where remineralization depth z_r is hold constant equal to 100 m. To take into account dependence of remineralization rate on ambient temperature, following (Segschneider and Bendtsen, 2013) we now use dependence of z_r on the thermocline temperature (300m) T:

$$z_r = z_{ro}\, 2^{\frac{T-T_0}{10}},$$

where T_0= 9°C and z_{ro}=100 m. The value of T_0 was selected such that introducing of temperature-dependent remineralization depth does not affect atmospheric CO_2 concentration under preindustrial climate conditions. During glacial times temperature in the thermocline decreases by 2-3°C which causes increase of z_r by 20-30%. This results in additional CO_2 drawdown by ca. 15 ppm.

A3. Variable volcanic outgassing

Following the idea by Huybers and Langmuir (2009) which has been tested already in Roth and Joos (2012), we introduced a dependence of volcanic CO_2 outgassing O on the rate of sea level change. Namely, we assume that volcanic outgassing linearly depends on sea level derivative with the time delay of about 5000 years:

$$O(t) = O_1\left(1 - O_2 \frac{dS(t-5000)}{dt}\right).$$

Here O_1=5.3 Tmol C yr^{-1}, and O_2=50 Tmol C m^{-1}. With these parameters volcanic outgassing does not change by more than 30% during all glacial cycles. Note, that over one glacial cycle the average value of O is very close to O_1.

Clim. Past Discuss., doi:10.5194/cp-2017-55, 2017
Manuscript under review for journal Clim. Past
Discussion started: 19 April 2017

A4. Modifications of the energy and surface mass balance interface

In our previous simulations with CLIMBER-2 we found that if maximum ice sheet volume in the Northern Hemisphere exceeds 100 m, the AMOC remains in the off mode during the entire deglaciation. Although it may be realistic for some recent deglaciations, such long AMOC shutdown prevents simulation of complete deglaciation of North America. This is related to the fact that due to a very coarse spatial resolution of CLIMBER-2 linear interpolation of surface temperature between neighbouring sectors (American and Atlantic) cause a strong cooling over eastern Part of Laurentide ice sheet doe to the AMOC shutdown (see for example Arz et al., 2007). In the high resolution climate models, the effect of AMOC shutdown on North America is rather limited compare to Europe (e.g. Zhang et al., 2014; Swingedouw et al., 2009). This is explained predominantly eastward direction of air masses transport. To compensate this resolution-related problem we made magnitude of temperature anomaly correction over eastern North America (see Fig. 2 in Ganopolski et al., 2010) dependent on the strength of the AMOC. Namely, for the AMOC strength below 10Sv, the amplitude of temperature correction is scaled down by factor $\Psi_{max}/10$, where Ψ_{max} is the maximum of the meridional overturning stream function (in Sv, 1 Sv=10^6 m^3/s) in the Atlantic Ocean. With this parameterization, during complete shutdown of the AMOC cooling over eastern North America is compensated by reducing of temperature correction. Introducing of this procedure minimizes the impact of the AMOC on Laurentide ice sheets mass balance. As the result, even prolonged AMOC shutdown does not prevent complete melting of the Laurentide ice sheet during glacial terminations.

Clim. Past Discuss., doi:10.5194/cp-2017-55, 2017
Manuscript under review for journal Clim. Past
Discussion started: 19 April 2017

Climate of the Past Discussions

Table 1. Model experiments performed in this study. P denotes prescribed characteristic, I - interactive, STD - standard model configuration, RD - variable remineralization depth, VO – variable volcanic outgassing, IF - iron fertilization in the South Ocean, TC – terrestrial carbon cycle, BR - brine rejection mechanism. Minus sign means that the process is excluded and plus sign means that process is included. Ice sheets are interactive in all simulations.

Experiment	Radiative forcing of GHGs	Southern Ocean dust	Atlantic freshwater factor	Modell configuration
		400,000 yr experiments		
ONE_1.0	P	P	1	STD
ONE_1.1	P	P	1.1	STD
ONE_S1	P	P	1.1	STD-RD
ONE_S2	P	P	1.1	STD-RD-VO
ONE_S3	P	P	1.1	STD-RD-VO-IF
ONE_S4	P	P	1.1	STD-RD-VO-IF-TC
ONE_240	240 ppm	P	1	STD
INTER_1.0	I	I	1	STD
INTER_1.1	I	I	1.1	STD
		130,000 yr experiments		
ONE_1.0_130K	P	P	1	STD
ONE_0.98_130K	P	P	0.98	STD
ONE_BRINE_130K	P	P	1	STD+BR

5

Clim. Past Discuss., doi:10.5194/cp-2017-55, 2017
Manuscript under review for journal Clim. Past
Discussion started: 19 April 2017

Climate of the Past Discussions

References

Abe-Ouchi, A., Saito, F., Kawamura, K., Raymo, M. E., Okuno, J., Takahashi, K., and Blatter, H.: Insolation-driven 100,000-year glacial cycles and hysteresis of ice-sheet volume, Nature, 500, 190-194, 10.1038/nature12374, 2013.

Adkins, J. F., McIntyre, K., and Schrag, D. P.: The salinity, temperature, and $\delta^{18}O$ of the glacial deep ocean, Science, 298, 1769-1773, 10.1126/science.1076252, 2002.

Archer, D., Winguth, A., Lea, D., and Mahowald, N.: What caused the glacial/interglacial atmospheric pCO_2 cycles?, Rev. Geophys., 38, 159-189, 10.1029/1999rg000066, 2000.

Arz, H. W., Lamy, F., Ganopolski, A., Nowaczyk, N., and Patzold, J.: Dominant Northern Hemisphere climate control over millennial-scale glacial sea-level variability, Quat. Sci. Rev., 26, 312-321, 10.1016/j.quascirev.2006.07.016, 2007.

Barnola, J. M., Raynaud, D., Korotkevich, Y. S., and Lorius, C.: Vostok ice core privides 160,000-year record of atmospheric CO_2, Nature, 329, 408-414, 10.1038/329408a0, 1987.

Berger, A., Li, X. S., and Loutre, M. F.: Modelling northern hemisphere ice volume over the last 3 Ma, Quat. Sci. Rev., 18, 1-11, 10.1016/s0277-3791(98)00033-x, 1999.

Bouttes, N., Paillard, D., and Roche, D. M.: Impact of brine-induced stratification on the glacial carbon cycle, Clim. Past., 6, 575-589, 10.5194/cp-6-575-2010, 2010.

Brady, E. C., Otto-Bliesner, B. L., Kay, J. E., and Rosenbloom, N.: Sensitivity to Glacial Forcing in the CCSM4, J. Clim., 26, 1901-1925, 10.1175/jcli-d-11-00416.1, 2013.

Brovkin, V., Ganopolski, A., and Svirezhev, Y.: A continuous climate-vegetation classification for use in climate-biosphere studies, Ecol. Model., 101, 251-261, 10.1016/s0304-3800(97)00049-5, 1997.

Brovkin, V., Hofmann, M., Bendtsen, J., and Ganopolski, A.: Ocean biology could control atmospheric $\delta^{13}C$ during glacial-interglacial cycle, Geochem. Geophys. Geosyst., 3, 15, 10.1029/2001gc000270, 2002.

Brovkin, V., Ganopolski, A., Archer, D., and Rahmstorf, S.: Lowering of glacial atmospheric CO_2 in response to changes in oceanic circulation and marine biogeochemistry, Paleoceanography, 22, 14, 10.1029/2006pa001380, 2007.

Brovkin, V., Ganopolski, A., Archer, D., and Munhoven, G.: Glacial CO_2 cycle as a succession of key physical and biogeochemical processes, Clim. Past., 8, 251-264, 10.5194/cp-8-251-2012, 2012.

Brovkin, V., Bruecher, T., Kleinen, T., Zaehle, S., Joos, F., Roth, R., Spahni, R., Schmitt, J., Fischer, H., Leuenberger, M., Stone, E. J., Ridgwell, A., Chappellaz, J., Kehrwald, N., Barbante, C., Blunier, T., and Jensen, D. D.: Comparative carbon cycle dynamics of the present and last interglacial, Quat. Sci. Rev., 137, 15-32, 10.1016/j.quascirev.2016.01.028, 2016.

Burley, J. M. A., and Katz, R. F.: Variations in mid-ocean ridge CO_2 emissions driven by glacial cycles, Earth Planet. Sci. Lett., 426, 246-258, 10.1016/j.epsl.2015.06.031, 2015.

Calov, R., Ganopolski, A., Claussen, M., Petoukhov, V., and Greve, R.: Transient simulation of the last glacial inception. Part I: glacial inception as a bifurcation in the climate system, Clim. Dyn., 24, 545-561, 10.1007/s00382-005-0007-6, 2005.

Ciais, P., Tagliabue, A., Cuntz, M., Bopp, L., Scholze, M., Hoffmann, G., Lourantou, A., Harrison, S. P., Prentice, I. C., Kelley, D. I., Koven, C., and Piao, S. L.: Large inert carbon pool in the terrestrial biosphere during the Last Glacial Maximum, Nat. Geosci., 5, 74-79, 10.1038/ngeo1324, 2012.

Crowley, T. J., and Hyde, W. T.: Transient nature of late Pleistocene climate variability, Nature, 456, 226-230, 10.1038/nature07365, 2008.

Fischer, H., Schmitt, J., Luthi, D., Stocker, T. F., Tschumi, T., Parekh, P., Joos, F., Köhler, P., Volker, C., Gersonde, R., Barbante, C., Le Floch, M., Raynaud, D., and Wolff, E.: The role of Southern Ocean processes in orbital and millennial CO_2 variations - A synthesis, Quat. Sci. Rev., 29, 193-205, 10.1016/j.quascirev.2009.06.007, 2010.

Freeman, E., Skinner, L. C., Waelbroeck, C., and Hodell, D.: Radiocarbon evidence for enhanced respired carbon storage in the Atlantic at the Last Glacial Maximum, Nat. Commun., 7, 8, 10.1038/ncomms11998, 2016.

Ganopolski, A., Petoukhov, V., Rahmstorf, S., Brovkin, V., Claussen, M., Eliseev, A., and Kubatzki, C.: CLIMBER-2: a climate system model of intermediate complexity. Part II: model sensitivity, Clim. Dyn., 17, 735-751, 10.1007/s003820000144, 2001.

Ganopolski, A., and Roche, D. M.: On the nature of lead-lag relationships during glacial-interglacial climate transitions, Quat. Sci. Rev., 28, 3361-3378, 10.1016/j.quascirev.2009.09.019, 2009.

Ganopolski, A., Calov, R., and Claussen, M.: Simulation of the last glacial cycle with a coupled climate ice-sheet model of intermediate complexity, Clim. Past., 6, 229-244, 2010.

Ganopolski, A., and Calov, R.: The role of orbital forcing, carbon dioxide and regolith in 100 kyr glacial cycles, Clim. Past., 7, 1415-1425, 10.5194/cp-7-1415-2011, 2011.

Ganopolski, A., Winkelmann, R., and Schellnhuber, H. J.: Critical insolation-CO_2 relation for diagnosing past and future glacial inception, Nature, 529, 200-204, 10.1038/nature16494, 2016.

Greve, R.: A continuum-mechanical formulation for shallow polythermal ice sheets, Philos. Trans. R. Soc. A-Math. Phys. Eng. Sci., 355, 921-974, 10.1098/rsta.1997.0050, 1997.

Hain, M. P., Sigman, D. M., and Haug, G. H.: Distinct roles of the Southern Ocean and North Atlantic in the deglacial atmospheric radiocarbon decline, Earth Planet. Sci. Lett., 394, 198-208, 10.1016/j.epsl.2014.03.020, 2014.

Huybers, P., and Langmuir, C.: Feedback between deglaciation, volcanism, and atmospheric CO_2, Earth Planet. Sci. Lett., 286, 479-491, 10.1016/j.epsl.2009.07.014, 2009.

Joos, F., Gerber, S., Prentice, I. C., Otto-Bliesner, B. L., and Valdes, P. J.: Transient simulations of Holocene atmospheric carbon dioxide and terrestrial carbon since the Last Glacial Maximum, Glob. Biogeochem. Cycle, 18, 20, 10.1029/2003gb002156, 2004.

Jouzel, J., Masson-Delmotte, V., Cattani, O., Dreyfus, G., Falourd, S., Hoffmann, G., Minster, B., Nouet, J., Barnola, J. M., Chappellaz, J., Fischer, H., Gallet, J. C., Johnsen, S., Leuenberger, M., Loulergue, L., Luethi, D., Oerter, H., Parrenin, F., Raisbeck, G., Raynaud, D., Schilt, A., Schwander, J., Selmo, E., Souchez, R., Spahni, R., Stauffer, B., Steffensen, J. P., Stenni, B., Stocker, T. F., Tison, J. L., Werner, M., and Wolff, E. W.: Orbital and millennial Antarctic climate variability over the past 800,000 years, Science, 317, 793-796, 10.1126/science.1141038, 2007.

Kaplan, J. O., Prentice, I. C., Knorr, W., and Valdes, P. J.: Modeling the dynamics of terrestrial carbon storage since the Last Glacial Maximum, Geophys. Res. Lett., 29, 4, 10.1029/2002gl015230, 2002.

Kleinen, T., Brovkin, V., and Munhoven, G.: Modelled interglacial carbon cycle dynamics during the Holocene, the Eemian and Marine Isotope Stage (MIS) 11, Clim. Past., 12, 2145-2160, 10.5194/cp-12-2145-2016, 2016.

Kobayashi, H., Abe-Ouchi, A., and Oka, A.: Role of Southern Ocean stratification in glacial atmospheric CO_2 reduction evaluated by a three-dimensional ocean general circulation model, Paleoceanography, 30, 1202-1216, 10.1002/2015pa002786, 2015.

Köhler, P., Fischer, H., and Schmitt, J.: Atmospheric $\delta^{13}CO_2$ and its relation to pCO_2 and deep ocean delta ^{13}C during the late Pleistocene, Paleoceanography, 25, 16, 10.1029/2008pa001703, 2010.

Kovaltsov, G. A., Mishev, A., and Usoskin, I. G.: A new model of cosmogenic production of radiocarbon C-14 in the atmosphere, Earth Planet. Sci. Lett., 337, 114-120, 10.1016/j.epsl.2012.05.036, 2012.

Lamy, F., Gersonde, R., Winckler, G., Esper, O., Jaeschke, A., Kuhn, G., Ullermann, J., Martinez-Garcia, A., Lambert, F., and Kilian, R.: Increased Dust Deposition in the Pacific Southern Ocean During Glacial Periods, Science, 343, 403-407, 10.1126/science.1245424, 2014.

Luthi, D., Le Floch, M., Bereiter, B., Blunier, T., Barnola, J. M., Siegenthaler, U., Raynaud, D., Jouzel, J., Fischer, H., Kawamura, K., and Stocker, T. F.: High-resolution carbon dioxide concentration record 650,000-800,000 years before present, Nature, 453, 379-382, 10.1038/nature06949, 2008.

Mahowald, N., Kohfeld, K., Hansson, M., Balkanski, Y., Harrison, S. P., Prentice, I. C., Schulz, M., and Rodhe, H.: Dust sources and deposition during the last glacial maximum and current climate: A comparison of model results with paleodata from ice cores and marine sediments, J. Geophys. Res.-Atmos., 104, 15895-15916, 10.1029/1999jd900084, 1999.

Mariotti, V., Paillard, D., Bopp, L., Roche, D. M., and Bouttes, N.: A coupled model for carbon and radiocarbon evolution during the last deglaciation, Geophys. Res. Lett., 43, 1306-1313, 10.1002/2015gl067489, 2016.

Martin, J. H.: Glacial-Interglacial CO_2 change: The iron hypothesis, Paleoceanography, 5, 1-13, 10.1029/PA005i001p00001, 1990.

Martinez-Garcia, A., Sigman, D. M., Ren, H. J., Anderson, R. F., Straub, M., Hodell, D. A., Jaccard, S. L., Eglinton, T. I., and Haug, G. H.: Iron Fertilization of the Subantarctic Ocean During the Last Ice Age, Science, 343, 1347-1350, 10.1126/science.1246848, 2014.

Menviel, L., Joos, F., and Ritz, S. P.: Simulating atmospheric CO_2, ^{13}C and the marine carbon cycle during the Last Glacial-Interglacial cycle: possible role for a deepening of the mean remineralization depth and an increase in the oceanic nutrient inventory, Quat. Sci. Rev., 56, 46-68, 10.1016/j.quascirev.2012.09.012, 2012.

Mignot, J., Ganopolski, A., and Levermann, A.: Atlantic subsurface temperatures: Response to a shutdown of the overturning circulation and consequences for its recovery, J. Clim., 20, 4884-4898, 10.1175/jcli4280.1, 2007.

Monnin, E., Steig, E. J., Siegenthaler, U., Kawamura, K., Schwander, J., Stauffer, B., Stocker, T. F., Morse, D. L., Barnola, J. M., Bellier, B., Raynaud, D., and Fischer, H.: Evidence for substantial accumulation rate variability in Antarctica during the Holocene, through synchronization of CO_2 in the Taylor Dome, Dome C and DML ice cores, Earth Planet. Sci. Lett., 224, 45-54, 10.1016/j.epsl.2004.05.007, 2004.

Opdyke, B. N., and Walker, J. C. G.: Return of the coral-reef hypothesis - basin to shelf partition of $CaCO_3$ and its effect on atmospheric CO_2, Geology, 20, 733-736, 10.1130/0091-7613, 1992.

Paillard, D.: The timing of Pleistocene glaciations from a simple multiple-state climate model, Nature, 391, 378-381, 10.1038/34891, 1998.

Peltier, W. R.: Global glacial isostasy and the surface of the ice-age earth: The ice-5G (VM2) model and grace, Annu. Rev. Earth Planet. Sci., 32, 111-149, 10.1146/annurev.earth.32.082503.144359, 2004.

Petit, J. R., Jouzel, J., Raynaud, D., Barkov, N. I., Barnola, J. M., Basile, I., Bender, M., Chappellaz, J., Davis, M., Delaygue, G., Delmotte, M., Kotlyakov, V. M., Legrand, M., Lipenkov, V. Y., Lorius, C., Pepin, L., Ritz, C., Saltzman, E., and Stievenard, M.: Climate and atmospheric history of the past 420,000 years from the Vostok ice core, Antarctica, Nature, 399, 429-436, 10.1038/20859, 1999.

Petoukhov, V., Ganopolski, A., Brovkin, V., Claussen, M., Eliseev, A., Kubatzki, C., and Rahmstorf, S.: CLIMBER-2: a climate system model of intermediate complexity. Part I: model description and performance for present climate, Clim. Dyn., 16, 1-17, 10.1007/pl00007919, 2000.

Prentice, I. C., Harrison, S. P., and Bartlein, P. J.: Global vegetation and terrestrial carbon cycle changes after the last ice age, New Phytol., 189, 988-998, 10.1111/j.1469-8137.2010.03620.x, 2011.

Reimer, P. J., Bard, E., Bayliss, A., Beck, J. W., Blackwell, P. G., Ramsey, C. B., Buck, C. E., Cheng, H., Edwards, R. L., Friedrich, M., Grootes, P. M., Guilderson, T. P., Haflidason, H., Hajdas, I., Hatte, C., Heaton, T. J., Hoffmann, D. L., Hogg, A. G., Hughen, K. A., Kaiser, K. F., Kromer, B., Manning, S. W., Niu, M., Reimer, R. W., Richards, D. A., Scott, E. M., Southon, J. R., Staff, R. A., Turney, C. S. M., and van der Plicht, J.: Intrcal13 and marine13 radiocarbon age calibration curves 0-50,000 years cal BP, Radiocarbon, 55, 1869-1887, 2013.

Roberts, J., Gottschalk, J., Skinner, L. C., Peck, V. L., Kender, S., Elderfield, H., Waelbroeck, C., Riveiros, N. V., and Hodell, D. A.: Evolution of South Atlantic density and chemical stratification across the last deglaciation, Proc. Natl. Acad. Sci. U. S. A., 113, 514-519, 10.1073/pnas.1511252113, 2016.

Roth, R., and Joos, F.: Model limits on the role of volcanic carbon emissions in regulating glacial-interglacial CO_2 variations, Earth Planet. Sci. Lett., 329, 141-149, 10.1016/j.epsl.2012.02.019, 2012.

Schmitt, J., Schneider, R., Elsig, J., Leuenberger, D., Lourantou, A., Chappellaz, J., Köhler, P., Joos, F., Stocker, T. F., Leuenberger, M., and Fischer, H.: Carbon Isotope Constraints on the Deglacial CO_2 Rise from Ice Cores, Science, 336, 711-714, 10.1126/science.1217161, 2012.

Segschneider, J., and Bendtsen, J.: Temperature-dependent remineralization in a warming ocean increases surface pCO_2 through changes in marine ecosystem composition, Glob. Biogeochem. Cycle, 27, 1214-1225, 10.1002/2013gb004684, 2013.

Sigman, D. M., and Boyle, E. A.: Glacial/interglacial variations in atmospheric carbon dioxide, Nature, 407, 859-869, 10.1038/35038000, 2000.

Spratt, R. M., and Lisiecki, L. E.: A Late Pleistocene sea level stack, Clim. Past., 12, 1079-1092, 10.5194/cp-12-1079-2016, 2016.

Stephens, B. B., and Keeling, R. F.: The influence of Antarctic sea ice on glacial-interglacial CO_2 variations, Nature, 404, 171-174, 10.1038/35004556, 2000.

Sugden, D. E., McCulloch, R. D., Bory, A. J. M., and Hein, A. S.: Influence of Patagonian glaciers on Antarctic dust deposition during the last glacial period, Nat. Geosci., 2, 281-285, 10.1038/ngeo474, 2009.

Swingedouw, D., Mignot, J., Braconnot, P., Mosquet, E., Kageyama, M., and Alkama, R.: Impact of Freshwater Release in the North Atlantic under Different Climate Conditions in an OAGCM, J. Clim., 22, 6377-6403, 10.1175/2009jcli3028.1, 2009.

Toggweiler, J. R., Russell, J. L., and Carson, S. R.: Midlatitude westerlies, atmospheric CO_2, and climate change during the ice ages, Paleoceanography, 21, 15, 10.1029/2005pa001154, 2006.

Waelbroeck, C., Labeyrie, L., Michel, E., Duplessy, J. C., McManus, J. F., Lambeck, K., Balbon, E., and Labracherie, M.: Sea-level and deep water temperature changes derived from benthic foraminifera isotopic records, Quat. Sci. Rev., 21, 295-305, 10.1016/s0277-3791(01)00101-9, 2002.

Wallmann, K., Schneider, B., and Sarnthein, M.: Effects of eustatic sea-level change, ocean dynamics, and nutrient utilization on atmospheric pCO_2 and seawater composition over the last 130 000 years: a model study, Clim. Past., 12, 339-375, 10.5194/cp-12-339-2016, 2016.

Watson, A. J., Bakker, D. C. E., Ridgwell, A. J., Boyd, P. W., and Law, C. S.: Effect of iron supply on Southern Ocean CO_2 uptake and implications for glacial atmospheric CO_2, Nature, 407, 730-733, 10.1038/35037561, 2000.

Watson, A. J., Vallis, G. K., and Nikurashin, M.: Southern Ocean buoyancy forcing of ocean ventilation and glacial atmospheric CO_2, Nat. Geosci., 8, 861-864, 10.1038/ngeo2538, 2015.

Willeit, M., Ganopolski, A., Calov, R., Robinson, A., and Maslin, M.: The role of CO2 decline for the onset of Northern Hemisphere glaciation, Quat. Sci. Rev., 119, 22-34, 10.1016/j.quascirev.2015.04.015, 2015.

Wolff, E. W., Fischer, H., Fundel, F., Ruth, U., Twarloh, B., Littot, G. C., Mulvaney, R., Rothlisberger, R., de Angelis, M., Boutron, C. F., Hansson, M., Jonsell, U., Hutterli, M. A., Lambert, F., Kaufmann, P., Stauffer, B., Stocker, T. F., Steffensen, J. P., Bigler, M., Siggaard-Andersen, M. L., Udisti, R., Becagli, S., Castellano, E., Severi, M., Wagenbach, D., Barbante, C., Gabrielli, P., and Gaspari, V.: Southern Ocean sea-ice extent, productivity and iron flux over the past eight glacial cycles, Nature, 440, 491-496, 10.1038/nature04614, 2006.

Wunsch, C.: Last Glacial Maximum and deglacial abyssal seawater oxygen isotopic ratios, Clim. Past., 12, 1281-1296, 10.5194/cp-12-1281-2016, 2016.

Zhang, X., Lohmann, G., Knorr, G., and Purcell, C.: Abrupt glacial climate shifts controlled by ice sheet changes, Nature, 512, 290-294, 10.1038/nature13592, 2014.

5

Clim. Past Discuss., doi:10.5194/cp-2017-55, 2017
Manuscript under review for journal Clim. Past
Discussion started: 19 April 2017

Climate of the Past Discussions
Open Access
EGU

Figures

a) **b)**

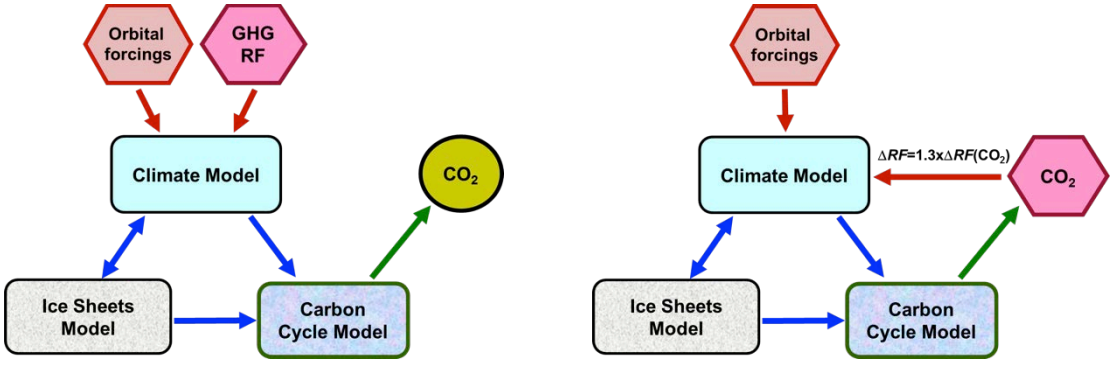

Figure 1. Coupling strategy. a) one-way coupled experiment; b) fully interactive experiment

Clim. Past Discuss., doi:10.5194/cp-2017-55, 2017
Manuscript under review for journal Clim. Past
Discussion started: 19 April 2017

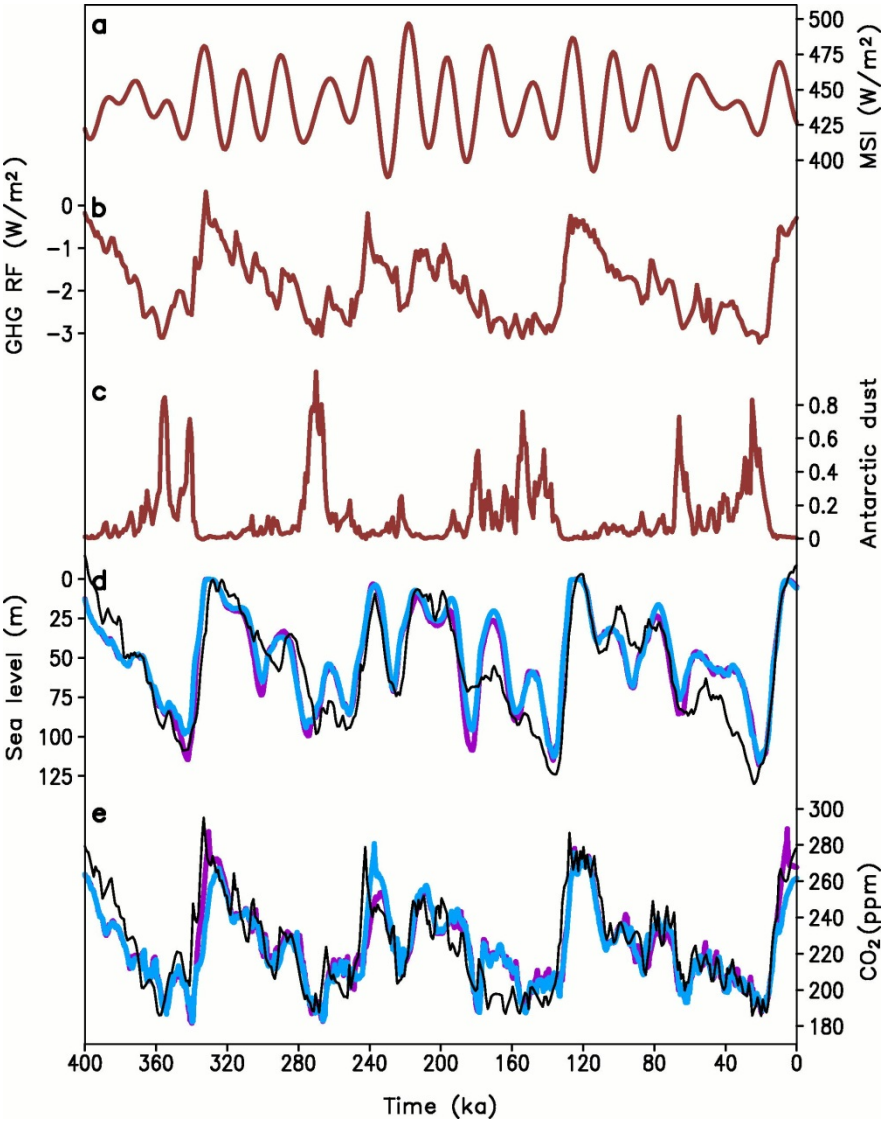

Figure 2. Transient simulations of the last four glacial cycles forced by orbital variations, observed concentration of well-mixed GHGs and dust deposition rate (one-way coupled experiments). a) Maximum summer insolation at 65°N, W/m^2; b) radiative forcing (relative to preindustrial) of well-mixed GHGs, W/m^2; c) Antarctic dust deposition rate in relative units; d) global ice volume expressed in sea level equivalent (m); e) atmospheric CO_2 concentration (ppm). Dark red colour in (a-c) represents prescribed forcings. Black lines in (d) is sea level stack from Spratt and Lisiecki (2016), in (e) compiled Antarctic CO_2 record from Lüthi et al. (2008). Blue lines in (d, e) correspond to the baseline experiment ONE_1.0 and pink lines to the experiment ONE_1.1 where meltwater flux into Atlantic was scaled up by factor 1.1.

Clim. Past Discuss., doi:10.5194/cp-2017-55, 2017
Manuscript under review for journal Clim. Past
Discussion started: 19 April 2017

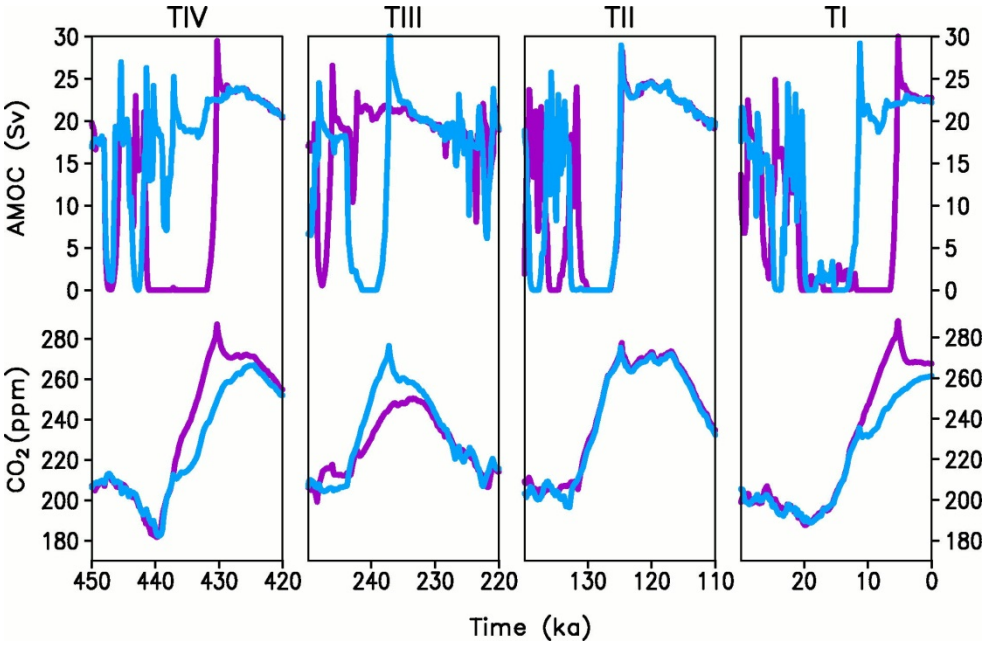

Figure 3. Temporal evolution of the AMOC, Sv (a), and atmospheric CO_2 concentration, ppm (b) during the last four glacial terminations. Blue lines correspond to the experiment ONE_1.0 and pink lines to the experiment ONE_1.1 where meltwater flux into Atlantic was scaled up by factor 1.1.

Clim. Past Discuss., doi:10.5194/cp-2017-55, 2017
Manuscript under review for journal Clim. Past
Discussion started: 19 April 2017

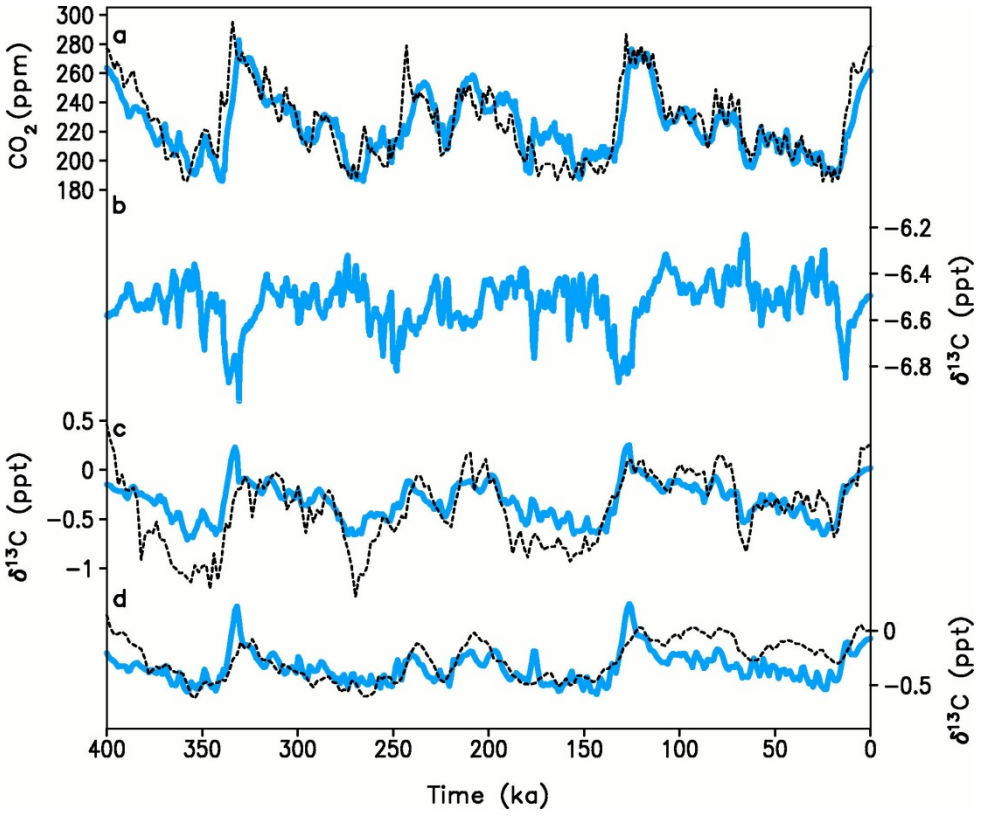

Figure 4. Simulated CO_2 and $\delta^{13}C$ with the one-way coupled model (ONE_1.0). a) CO_2 concentration (ppm) ref, b) atmospheric $\delta^{13}CO_2$ (‰), c) deep South Atlantic $\delta^{13}C$ (‰); d) deep North Pacific $\delta^{13}C$ (‰), (Lisiecki et al., 2008). Blue lines – model results, black dashed lines - empirical data.

Clim. Past Discuss., doi:10.5194/cp-2017-55, 2017
Manuscript under review for journal Clim. Past
Discussion started: 19 April 2017

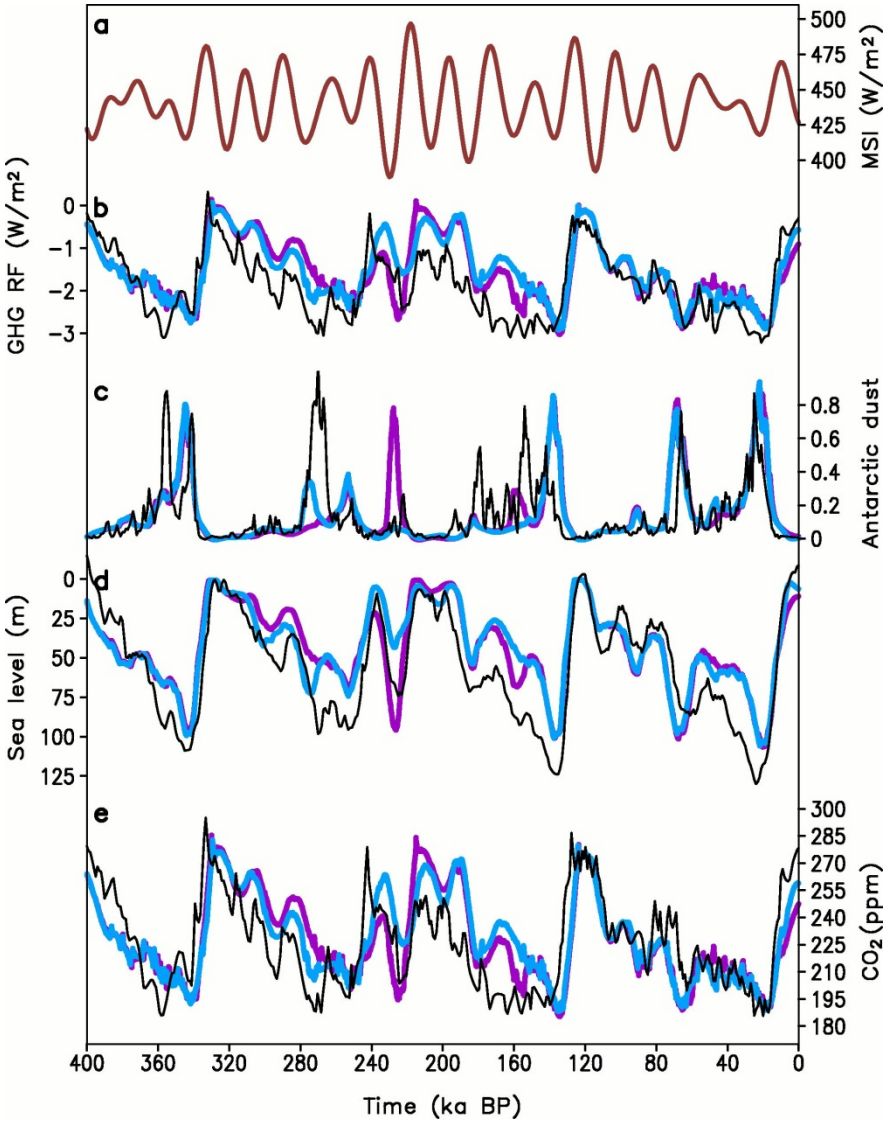

Figure 5. Transient simulations of the last four glacial cycles forced by orbital variations only (fully interactive experiments) a) Maximum summer insolation at 65°N, W/m^2; b) radiative forcing (relative to preindustrial) of well-mixed GHGs, W/m^2; c) Antarctic dust deposition rate in relative units; d) global ice volume expressed in sea level equivalent, m; e) atmospheric CO_2 concentration, ppm. Black lines in (b) and (c) are as forcings in Fig.2; (d) and (e) as data in Fig. 2. Blue lines in (d,e) correspond to the fully interactive experiment INTER_1. and pink lines to the experiment INTER_1.1 where meltwater flux into Atlantic was scaled up by factor 1.1.

Clim. Past Discuss., doi:10.5194/cp-2017-55, 2017
Manuscript under review for journal Clim. Past
Discussion started: 19 April 2017

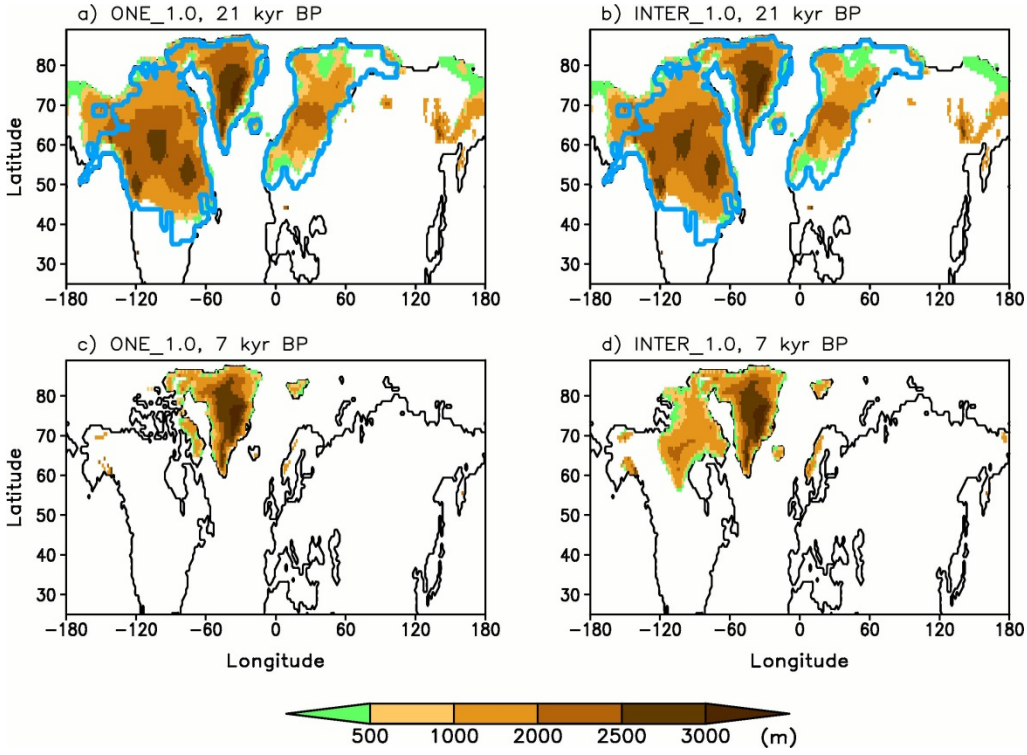

Figure 6. Simulated ice sheets elevation, m, at 21 ka (a, b) and 7 ka (c,d) in the one-way coupled experiment ONE-1.0 (a, c) and fully interactive experiment INTER-1.0 (b, d). Blue lines represent Ice-5g reconstruction at the LGM (Peltier, 2004).

Clim. Past Discuss., doi:10.5194/cp-2017-55, 2017
Manuscript under review for journal Clim. Past
Discussion started: 19 April 2017

Climate of the Past Discussions

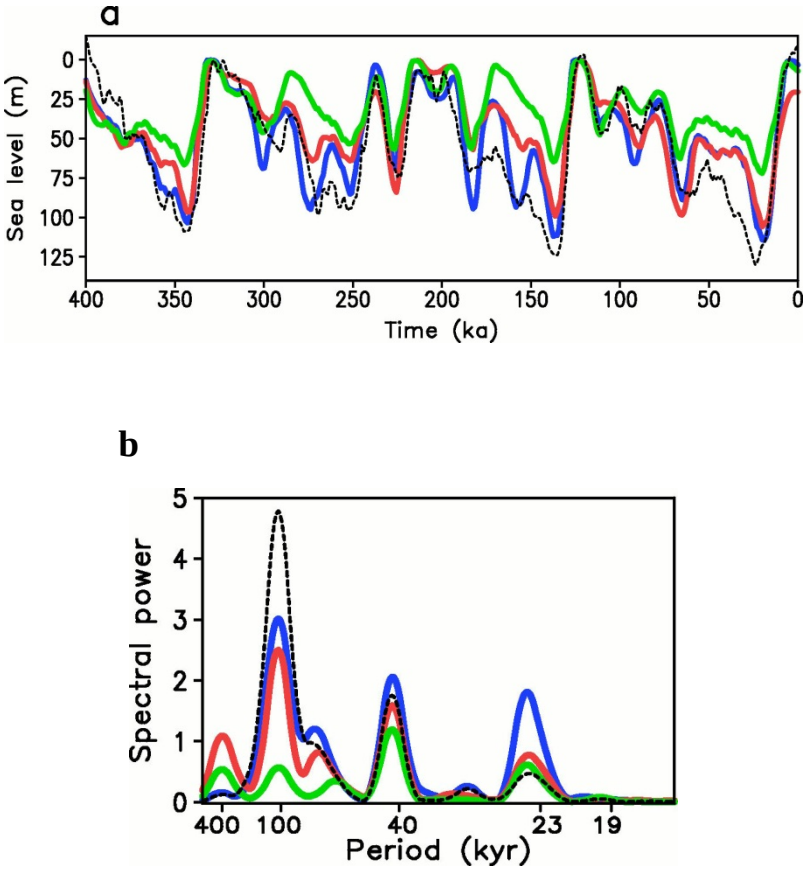

Figure 7. (a) Temporal evolution of reconstructed and simulated sea level, m; (b) their frequency spectra, kyr. Black line is for the data (Spratt and Lisiecki , 2016), blue line corresponds to the one-way coupled experiment ONE_1.0, red line to the fully interactive experiment INTER_1.0, and green line to the ONE_240 experiment with constant (240 ppm) CO_2 concentration.

Clim. Past Discuss., doi:10.5194/cp-2017-55, 2017
Manuscript under review for journal Clim. Past
Discussion started: 19 April 2017

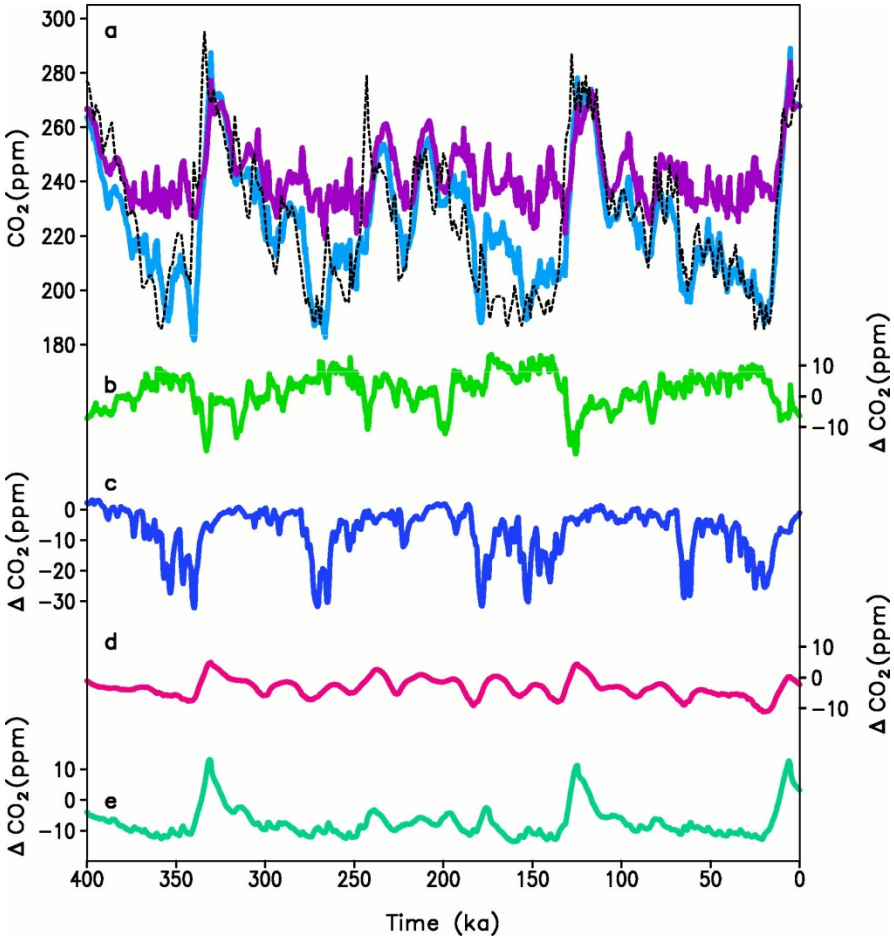

Figure 8. Results of factor separation analysis. a) Simulated CO_2 (ppm) in one-way coupled ONE_1.1 experiment (blue line), simulation ONE_S4 which do not include effects of iron fertilization, variable volcanic outgassing and temperature-dependent remineralization depth (pink line); and reconstructed CO_2 concentrations (black dashed line, Lüthi et al., 2008). b-d): contributions to simulated atmospheric CO_2 (ppm) of terrestrial carbon cycle (b), ONE_S4 – ONE_S3; iron fertilization (c), ONE_S3 – ONE_S2; variable volcanic outgassing (d), ONE_S2 – ONE_S1; temperature-dependent remineralization depth (e), ONE_S1 – ONE_1.1.

Clim. Past Discuss., doi:10.5194/cp-2017-55, 2017
Manuscript under review for journal Clim. Past
Discussion started: 19 April 2017

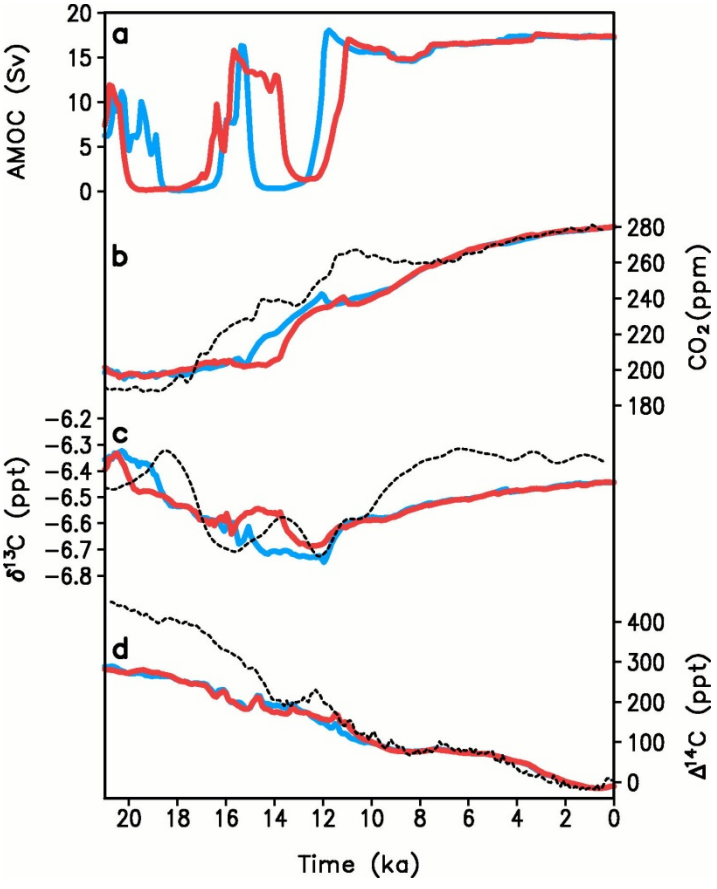

Figure 9. Simulation of Termination I with the set of one-way coupled models which differs only by scaling of freshwater flux. Blue line corresponds to the ONE_0.98_130K experiment with scaling factor 0.98, red line – the ONE_1.0_130K experiment with scaling factor 1.0. a) AMOC strength, Sv; b) atmospheric CO_2, ppm; c) $\delta^{13}CO_2$, ‰; d) $\Delta^{14}CO_2$, ‰. Dashed lines: b-c) ice-core data (Lüthi et al., 2008; Schmitt et al, 2012); d) IntCal13 radiocarbon calibration curve (Reimer et al. 2013).

Clim. Past Discuss., doi:10.5194/cp-2017-55, 2017
Manuscript under review for journal Clim. Past
Discussion started: 19 April 2017

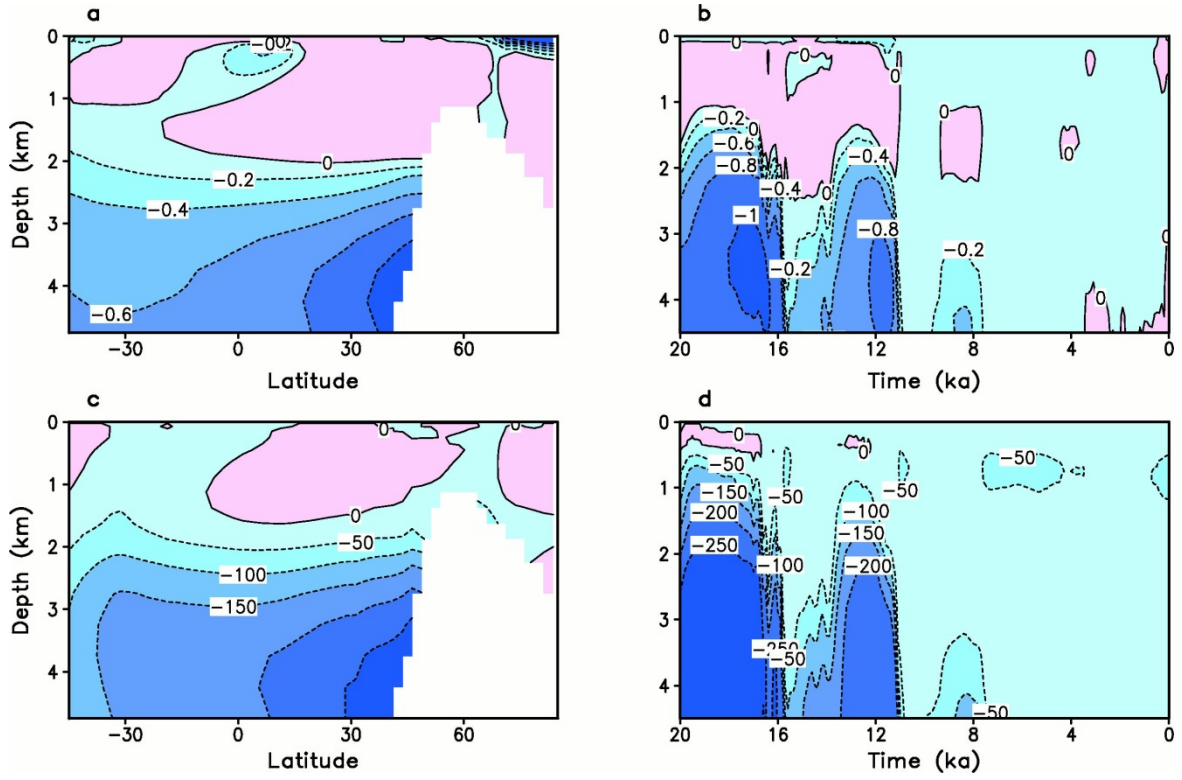

Figure 10. Carbon isotopes distribution in the Atlantic ocean in the ONE_1.0_130K simulation of Termination I. (a, b) $\delta^{13}C$, ‰, (c, d) $\Delta^{14}C$ in ‰. (a, c) differences between LGM (21 ka) and pre-industrial in the Atlantic ocean. (b, d) temporal evolution of anomalies during the past 20 ka at 20°N in Atlantic. For $\Delta^{14}C$, differences between given depth and mixed layer $\Delta^{14}C$ are shown.

Clim. Past Discuss., doi:10.5194/cp-2017-55, 2017
Manuscript under review for journal Clim. Past
Discussion started: 19 April 2017

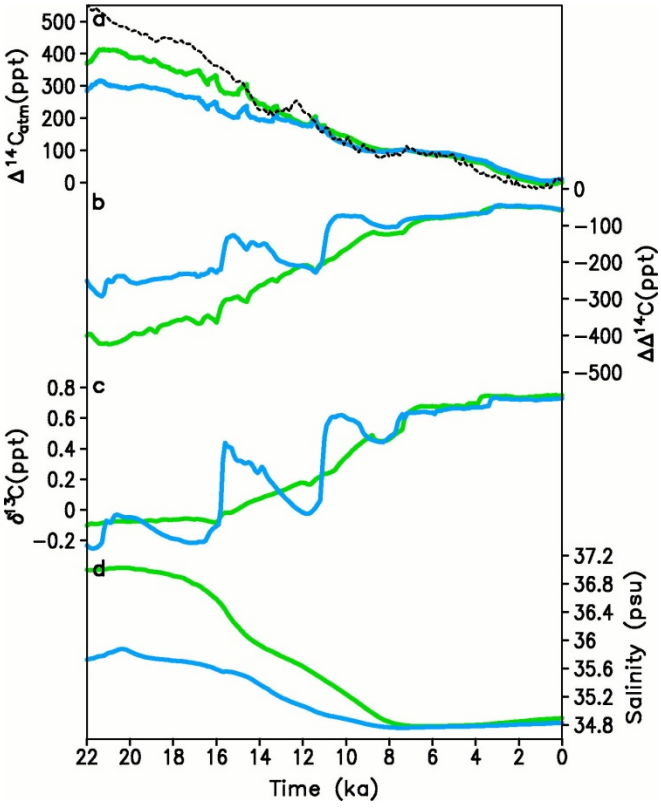

Figure 11. Simulation of Termination I in the standard ONE_1.0_130K experiment (blue) and the ONE_BRINE_130K experiment which includes brine parameterization and stratification-dependent vertical mixing (g). (a) atmospheric $\Delta^{14}C$ (in ‰). (b) Deep tropical Atlantic $\Delta\Delta^{14}C$, ‰. (c) Deep tropical Atlantic $\delta^{13}C$, ‰. (d) Deep Southern Ocean salinity, psu. (c-d) are for the depth 4 km. Black dashed line is IntCal13 radiocarbon calibration curve (Reimer et al. 2013).

Clim. Past Discuss., doi:10.5194/cp-2017-55, 2017
Manuscript under review for journal Clim. Past
Discussion started: 19 April 2017

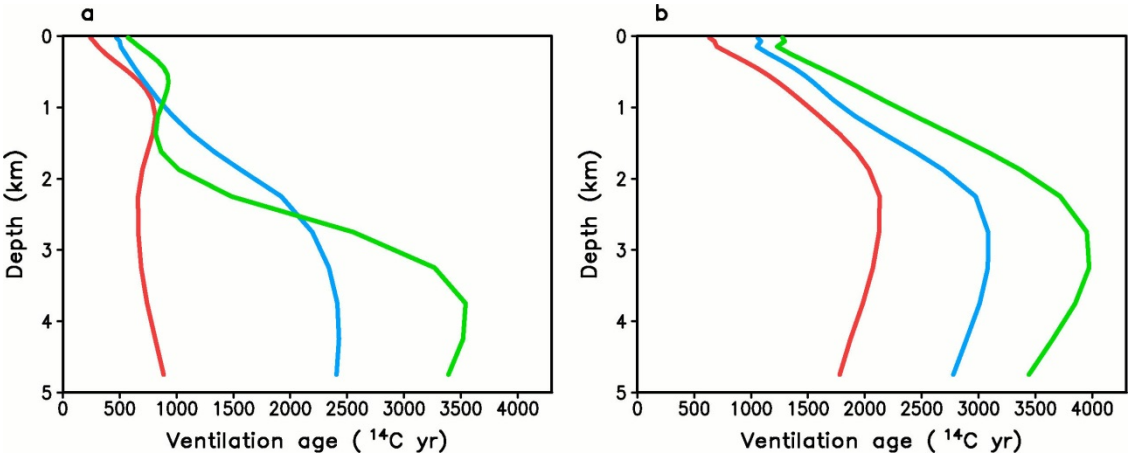

Figure 12. Vertical profile of ventilation age in ^{14}C years for Atlantic (a) and Pacific (b). Red line represents modern conditions, blue – LGM in ONE_1.0_130K experiment using the standard version of the model, green – LGM in ONE_BRINE_130K experiment with the model version which includes brine parameterization and stratification-dependent vertical mixing.

Clim. Past Discuss., doi:10.5194/cp-2017-55, 2017
Manuscript under review for journal Clim. Past
Discussion started: 19 April 2017

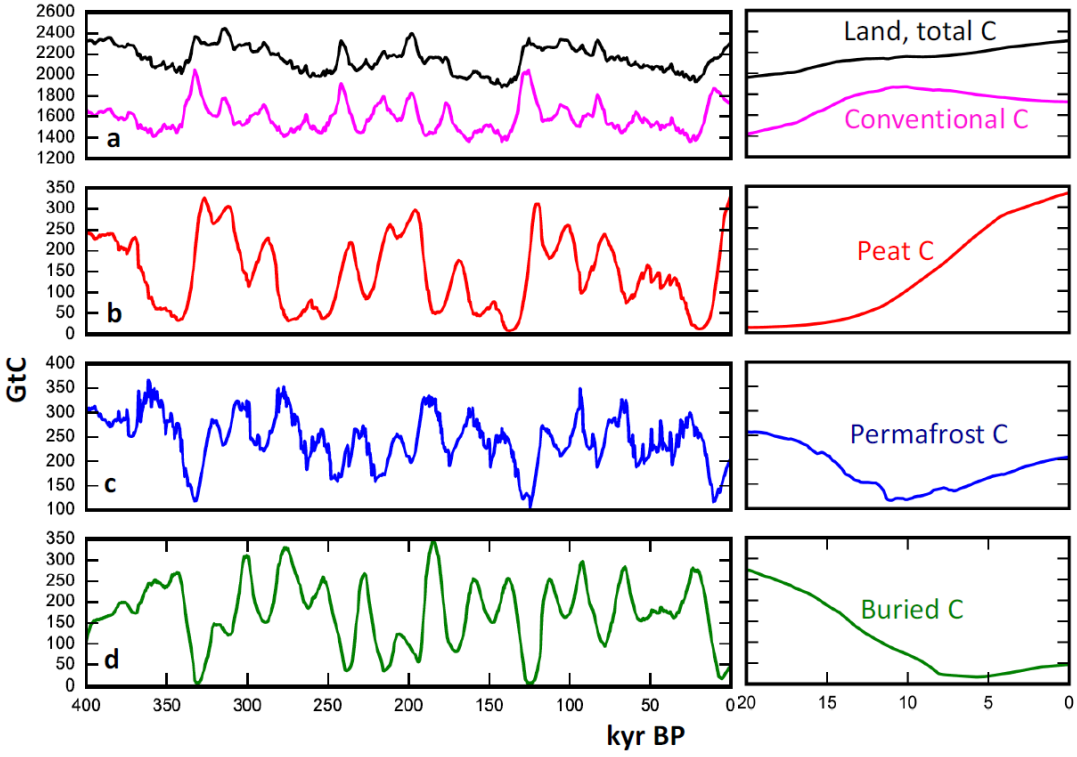

Figure 13. Dynamics of terrestrial carbon pools (Gt C) in the one-way coupled ONE_1.0 simulation. Left, the whole 400 kyr period; right, the Termination I period. a) Black line – total carbon storage; magenta line - conventional carbon pools (biomass and mineral soils), b-d: peat, permafrost, and buried carbon storages, respectively.

Clim. Past Discuss., doi:10.5194/cp-2017-55, 2017
Manuscript under review for journal Clim. Past
Discussion started: 19 April 2017

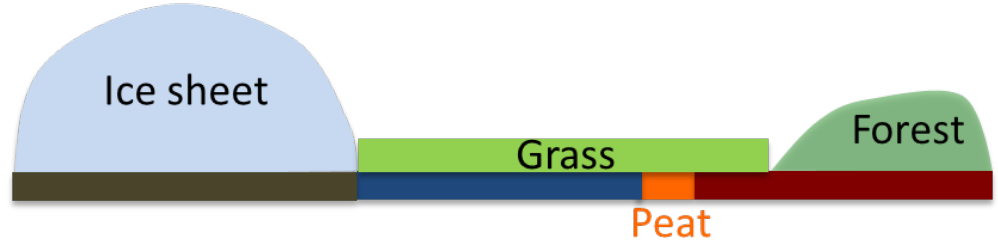

Figure A1. A sketch of distribution of soil carbon pools in the model.